Author Final Response

acp-2021-950

We are very grateful to the three referees for their detailed and fruitful comments which have allowed us to clarify various points. We copy-pasted below their reviews. Comments from Reviewers #1, #2 and #3 are in blue, red and green, respectively. For each comment/suggestion, our responses are in bold black and quotes from the revised text are in italic black. We also provide a track-change manuscript at the end of the present document.

General comments

The necessity of this paper apparently appeared when the authors performed their first inversion (presented in the Supplement). As a result, the paper is a bit unbalanced and thin in content. The title promises "atmospheric inversions", but the main paper only presents forward simulations as a series of sensitivity simulations to map out the impact of various choices for the Cl field. I therefore suggest to remove "through atmospheric inversions from the title".

The question posed in the title is interesting, but can it strictly speaking be answered based on this study, as the results are based on the forward simulations?

In the revised manuscript, we performed, for each sensitivity test, real atmospheric inversions with the 3-D variational inversion system developed by Thanwerdas et al. (2021) (M1 method) as well as with a simpler analytical inversion system and a one-box model mathematical framework (M2 method) . We also corrected our original method (M3 in the revised manuscript) to take account of the referees' recommendations. We therefore present three methods, from the more robust and computationally-expensive one (M1) to the less computationally-expensive one (M3). The methods are briefly explained in Sect. 2.5 and in more detail in the supplement (Text S1, S2 and S3).

With these changes, we think that keeping "through atmospheric inversions" is relevant.

The box model inversions are an elegant way to estimate the global impact of the Cl sink on emissions and their required signature. However, the comparison to the vertical profiles are only performed for CH_4 mixing ratios. The results indicate that the model does not perform very well, but that this is likely a transport issue rather than an issue with the Cl sink. However, it remains totally unclear how well the model performs in the stratosphere concerning $\delta^{13}C(CH_4)$, while the action of Cl is critical here. I therefore suggest to include an analysis of the modeled $\delta^{13}C(CH_4)$ profiles and compare to the available observations

We thank the referee for qualifying our method as elegant. We agree with the comments on $\delta^{13}C(CH_4)$ vertical profiles and we added a comparison with observations from Rockmann et al. (2011) in Sect. 3.7.

Whilst I find the idea of such quantification useful (nothing innovative but another set of simulations will add to statistic and perhaps could thus help quantifying the uncertainties about other AC-GCM/CTM-specific terms, e.g. dynamics), no marked advance in Cl-CH_4 interaction in the atmosphere is obtained, plus the analysis offered ruins the attempt. I foremost imply Section 3.2 (after which I could not continue with required scrutiny) which introduces very questionable "fit methodology" (see the general comment below).

One has to consider that many recent inversion studies on the CH$_4$ cycle do not include the full Cl sink in their setup. This is an issue to properly close the global methane budget using top-down approaches, especially when assimilating isotopic observations. So, documenting in this paper the influence of the Cl sink with an inversion perspective seems a necessary and important step. Indeed, if we do not bring advances in the Cl-CH$_4$ chemical interaction with our work, it aims at providing more data and statistics to the scientific debate about all uncertainties existing in top-down estimates of the global methane budget.

We apologize for not making our methodology more robust and maybe clearer. In the revised manuscript, we included two additional methods that are more robust but more computationally-expensive compared to the original box-model approach. Furthermore, we showed that the original box-model method, with your suggested modifications, provides results that are highly consistent with more robust methods. We hope that this revised manuscript will answer your concerns on the methodology.

Even provided that this is repaired, my other major concern (seconding the Reviewer #1) is in that the study is largely based on results of another – to date not peer-review-completed – study by the same first and another four authors. It is necessary that the latter is finally reviewed in order to be certain that CH$_4$ fluxes used in the simulations are adequate. After that, my suggestion is to consider resubmission of the current work to the GMD, as this journal appears to be more appropriate for the content presented. Compared to other manuscripts submitted to Copernicus journals by Thanwerdas et al. recently, the current one is somewhat better in terms of composition and information content but not sufficiently clearer in conveying the story and presenting methods and discussion (see the specific/presentation comments below). The authors still have to put a considerable effort in improving this.

The study on which our results are largely based (Thanwerdas et al., 2021) has been accepted very recently for publication in the GMD journal after very minor peer-reviewing comments. The process was very long because the topical editor was unable to find reviewers, and not because comments were major. See the link below.
https://gmd.copernicus.org/preprints/gmd-2021-106/

We do think ACP is more appropriate for such a paper as the entire community of atmospheric inversion could benefit from such an analysis that is not uniquely related to model development but also implies quantitative results regarding the global methane sinks and budget. Although this work is based on the LMDz-SACS model, the approach and results are very likely to be similar with other chemistry-transport models. We indeed put a large effort into producing this updated version, answering all reviewers' comments, which allowed us to largely clarify and improve the rendering of our work.

I am not fine with the averaging of absolute biases (in both surface- and column-wise comparisons) – their average may be spuriously reduced through the summation of negative and positive members. Thus obtained low global mean biases do not guarantee that local (per-station or per-altitude) biases are at their optimum. Also, an indication that Cl spatial distribution is wrong will be lost. As a remedy, use squares of biases (as conventionally used in, e.g., least-square fit); I also suggest not to use latitudinal averaging due to the same reasons.

Line 237. Is it justified to use mean bias in the comparisons? Positive and negative biases (time, latitude or vertical) will cancel out to some extent.

To analyze the surface biases in the first version, we preferred to use mean biases because they were easier to interpret than root-mean square differences and because all values included in one average were either all positive or all negative.

However, following your relevant suggestions, we used square of biases (root-mean squared differences, RMSD) to perform our analysis in the revised manuscript. This modification affected the numerical values, especially for vertical profiles but did not affect our conclusions. We also removed any latitudinal averaging, mainly owing to a change in the methodology.

What is meant by "temporal evolution of CH_4 budget is not linear"? If you state that sink is proportional to CH_4 abundance, how can both decrease/increase introduce both negative feedback? What feedback is meant here?

Lines 245-247. What is meant by negative feedback from both decrease and increase?
"CH_4 decrease/increase induces a negative feedback on the magnitude of the sink, leading to a stabilization of the mass of CH_4 after several decades if S and тi are constant over time."

This sentence has been clarified and is now in the supplement (Text S3).

"If the total mass of CH_4 is increasing in response to a flux enhancement, the total sink will also increase and lead to a stabilization of the total mass after several decades."

A negative feedback was referring here to a feedback that occurs when a process is fed back in a manner that tends to reduce the fluctuations of this same process. Here, the increase in atmospheric methane in response to a flux enhancement causes the sink to increase and therefore the atmospheric methane mole fractions to stabilize. In a similar way, the decrease in atmospheric methane in response to a flux reduction causes the sink to decrease and therefore the atmospheric methane mole fractions to stabilize. In both cases, this is negative feedback.

"Decrease / increase" was just referring to the fact that both a decrease and an increase in atmospheric CH_4 mole fractions lead to a negative feedback resulting from a change in the total sink.

You perform simulations with varying CH_4 emissions and sinks (biases are derived for varying S and τ_i) yet you assume S ant τ_i constant over time in the analysis. How valid is this approach? How large are the errors introduced by this assumption?

Note that, in the revised manuscript, the methodology the referee is commenting on is only one of the three methods that are used. It is now called M3 for "method 3". We apologize for not making our assumption clearer. In fact, we do not need to assume S constant. Only ΔS and $τ_i$ must be assumed constant. As the contribution of the Cl sink to the total sink, the interannual variability of the Cl sink and the interannual variability of the atmospheric lifetime are very low, it is not a strong assumption. These assumptions are further discussed in Text S3.

In the revised manuscript, we use two other methods that are more robust and we show that M3 is providing results that are very consistent with the other methods. The discrepancies between M3 and M1 mean results, which are the most robust results that we can provide, are below 10 %.

Why inventing a cumbersome apparatus when you can simply diagnose changes in sink terms (hence ΔS) directly from the simulations? If you still like to use the "box-model" apparatus, why not writing solutions for Eq. 3 for each simulation and their differences (read biases) in analytical form? Ultimately, you confuse the Reader (and yourself) so much that in Eq. 7 you fit both A and B parameters. On which grounds? B represents τ_ref and should be the same for all simulations (it is from a reference simulation, isn't it?) At t→ (steady state), Eq. 6 reduces to b(t)=ΔS´τ_ref. Using the biases from Table 5, this yields various τ_ref for different simulations (about 8 yrs for three of them and 12 yrs for the rest!), how do you explain that? My explanation is that by

fitting A and B simultaneously you receive their whatever combination that minimises error-prone averaged absolute biases in the first two decades of simulations. What is the value of τ_ref in the reference simulation?

It appears to us that we cannot use changes in sink terms (ΔP) to infer ΔS. ΔP increases throughout the time period, starting from zero at the beginning of the period to a maximum value at the end of a very long period of stabilization. Should we use the maximum value of ΔP, an average over the time period or something else ? Also, should we use the tropospheric sink or total sink ? We think it is better to directly diagnose ΔS from the biases in atmospheric mole fractions as we can also capture the influence of the stratospheric sink on mole fractions at the surface. In the revised manuscript we changed the presentation of this method (see Text S3 in the supplement) and applied some of your suggestions.

We agree that τ_ref should be the same for all simulations to avoid fitting two terms simultaneously. As you pointed out, using two terms results in very different lifetimes, sometimes not consistent with data. In the revised version, we therefore use τ_ref as taken from the CI-Wang simulation (reference).

Same argumentation as for Sect. 3.2 applies, plus you have to show how the fitting is done for isotope ratios, specifically how $\delta^{13}C$ biases are obtained. In any case, regarding the erroneous fitting of total CH_4, I suspect same or greater problems with $^{12}CH_4$ and $^{13}CH_4$.

Lines 286-288. How should B be interpreted when fitting eq(6) for $\delta^{13}C$ methane?

Applying our methodology directly to $\delta^{13}C(CH_4)$ biases was not a good idea and the B factor in Eq. 7 was indeed very difficult to interpret.

In the revised manuscript, we use the method M3 (original method in the submitted paper) on both $^{12}CH_4$ and $^{13}CH_4$ simulated tracers and not directly on $\delta^{13}C(CH_4)$. Furthermore, we analyze the biases in total mass rather than the biases in mole fractions. This way, we can directly infer ΔS in $TgCH_4.yr^{-1}$ without using a conversion factor and we do not need any bias averaging.

Using this revised method, we infer a ΔS for both $^{12}CH_4$ and $^{13}CH_4$ (ΔS_{12} and ΔS_{13}) and deduce a $\Delta\delta^{13}C(CH_4)_{source}$ based on these two values. As shown in Sect. 3.4 and Figure 3, it provides results that are very consistent with the more robust methods included in the revised version of the manuscript (M1 and M2).

267 Why not using a conversion factor derived directly from your model simulations? You are using a factor from a study employing a model actual for early 1990s using a very different OH field (Spivakovsky climatology) and meteorology. You may introduce an error in conversion larger than that of any other assumptions used…

Lines 266-268. Is it justified to use the conversion factor of Lassey et al 2000? The distribution of sinks and the resulting methane distribution will affect the conversion factor between mixing ratio and emissions.

We agree with these comments.

For the original method, now M3, we changed the methodology and now analyze the biases in total mass rather than the biases in mole fractions. It allows us to directly infer in $TgCH_4.yr^{-1}$ without using a conversion factor. The new method is comprehensively described in Text S3 in the supplement.

However, we still use a conversion factor in the new method M2 to convert a total atmospheric mass of CH_4 to a CH_4 mole fraction at the surface. This conversion factor is now directly derived from our simulations. The method M2 is comprehensively described in Text S2 in the supplement.

"To compare the total atmospheric CH$_4$ mass and the observed CH$_4$ mole fraction at the surface, we use a conversion factor in TgCH$_4$.ppb^{-1} that is calculated using the outputs of the forward simulations (FWD-*) and by dividing the tracer total mass by the tropospheric mass-weighted average of mole fractions."

It would be beneficial for the paper to briefly review the processes included in the models and possible differences between the models. Now the discussion is on a very general level, e.g., lines 61-64 "...have made important developments in tropospheric chemistry modeling...".

We agree with this comment and included more details on the differences between the models/simulations in Sect. 2.1 and 2.2.

For completeness, the photolysis of methane could be added to the reactions (Table 2) as the model extends to ca. 75 km, even though it would likely not impact any of the results in this study.

We agree with this comment. However, the inversions performed with our model never included the photolysis of methane because it was considered negligible. Also, none of the inversion studies mentioned in the introduction, in particular those of Saunois et al. (2020), accounted for this sink in the upper atmosphere. Adding this process to our simulations would require a lot of time (implementation and tests) for a result that is very likely to not impact the results of our study, and more generally of surface inversions. In the revised manuscript, we included this explanation in Sect. 2.1.

Lines 135-136. "More details on the modeling of this field are available in the supplement." However, there are not really any further details given on the simulation, practically the same text is given on lines 120-128 as in the supplement lines 49-60, really the only addition is Table S3. Also, table S3 is almost a duplicate of Table 1 in the manuscript, only the sink column and the average KIE is added to table S3 compared to Table 1. Table S3 seems redundant.

We apologize for this mistake. We removed the text in the supplement about the Cl-INCA field as we now provide an explanation of the differences between the models that generated the tested Cl fields in Sect. 2.2.. Table S3 was originally added to provide some information about the global KIE that could be useful to one-box modelers. However, we agree that is not very relevant for this study and we therefore removed the Table.

Lines 135-140. The main missing reactions/processes could be mentioned.

We now mention this in the discussion in Sect. 2.2.

Lines 169-176, Scaling the Cl-INCA field to match the tropospheric average of Cl in the ClWang field may introduce some differences, at least visually it seems like the Cl fields would differ at high latitudes, even though the tropospheric average would be nearly the same.

We do not use the scaling anymore in the revised methodology. The Cl-Wang field is directly prescribed.

Overall, it would be relevant to have an overview of the major differences between the simulations. The global average is interesting, but the latitudinal and vertical distributions are also important for understanding the impact. Here it would be beneficial to have an overview of the model differences, e.g., the Cl-INCA field seems to have a low (or missing) release of Cl from sea-salt aerosols (Figure 1). Elevated halogen concentrations are often observed in the spring at high latitudes, which could affect surface C13 methane concentrations observed at high latitude stations etc. Latitudinal differences in the Cl field would also cause different responses in the source estimates an inversion system.

We agree on this point and in the revised manuscript, we provide more information about the spatial differences between simulations (e.g. in Sect. 3.2) and the impacts of these spatial differences on top-down estimates (Sect. 3.3 and 3.4).

Section 2.3. The setup, if I understood correctly, is based on an inversion using a Cl burden that is about half of the one used in the forward run, SimREF, that is then used as reference for the other forward runs using different Cl fields. The fluxes are therefore not optimized with the same Cl burden as in the SimREF, but nevertheless SimREF is used as reference for deriving the delta S, i.e., the source change required to adjust for the different loss rates in the different simulations. The total fluxes would not be affected much, but the distribution between the source categories could be affected. This should be elaborated.

We changed the methodology in the revised manuscript. Now, there is one inversion (INV-*) for each Cl-field resulting in multiple sets of optimized fluxes and isotopic source signatures. There is also one forward simulation for each Cl-field (FWD-*) with, this time, the same optimized fluxes and source signatures taken from INV-Wang. This methodology is more consistent and does not use scaled Cl fields as before.

The distribution between the source categories (source mixture) is indeed modified because the inversion system needs to modify the globally-averaged isotopic signature of the total source of CH_4. We included results and discussion on this matter in Sect. 3.4.

Lines 234-236. Should the SimREF be validated more rigorously when it is used as reference for the other simulations? If the SimREF has biases compared to observations, it might affect the conclusions from the box model analysis (delta S).

In the revised manuscript, we perform a 3-D variational inversion for each Cl field. We therefore cannot be more consistent with the observational data and provide more robust estimates of the Cl influence on top-down estimates.

Lines 241-264. The reason for the introduction of the box model analysis is somewhat unclear. It seems that the driver data ended before the models reached steady state, therefore the steady state had to be estimated by the fitting procedure derived using the box model approach. A more straightforward alternative would be to repeat the simulated years until steady state is reached. The seasonal and interannual variability in the bias, seen in Fig 2, is relatively small compared to the bias. Therefore, it would be justified to repeat the same years to reach steady state. The steady state values could then be used in the analysis instead of fitted values. What is the information obtained in the fitting procedure from B in eq(6)? The values of B are not shown, but they should be almost identical for the different fits? Are they realistic?

The ultimate goal of this approach is to reduce the computational burden of comparing the influences of two Cl fields on top-down estimates. Repeating the same years would require to perform the simulation over 70 years, therefore three times more than what we did. Our original method (now M3) provides results which proved to be very consistent with other methods, assuredly more robust (M1 and M2), at a reasonable computational cost. We therefore think that this compromise is acceptable and avoid doing a simulation spanning 70 years. Also, we improved the methodology of M3 and we now use the total mass in the atmosphere rather than the globally-averaged tropospheric mole fraction to perform the fitting procedure and estimating ΔS. We think it is more relevant as it does not require any averaging, only a sum.

Lines 268-269. "For SimNoCl and SimSherwen, these estimations are very close (difference of less than 0.2 $TgCH_4 \cdot yr^{-1}$) to the tropospheric Cl sink discrepancies from Table 4." Maybe the authors meant SimNoTropo? Then the discussion in the following lines is more understandable.

SimSherwen: 9.9-3.2=6.7 from Table 4 vs. 6.6 in Table 5
SimNoCl: 0-3.2=-3.2 from Table 4 vs. -5.7 in Table 5
SimNoTropo: 0-3.2=-3.2 from Table 4 vs. -3.2 in Table 5

Yes, we meant SimNotropo. We apologize for this mistake. This section has however been largely modified and this specific sentence has been removed.

Table 5. Latitudinal dependency is reported as min/max, but it is unclear which latitude band is associated with which value.

We no longer use latitudinal averages because our methodology has been modified. Also, Table 5 has been removed.

Lines 298-302. The value for SimREF, -52.6 from table 2, could be given here to aid the reader. Oscillate is not a good choice of word here, the value does not oscillate, it just depends on the simulation.

We largely modified this section and we now discuss the range of globally-averaged source signatures in Sect. 3.4. We agree that the word 'oscillate' was not a good choice.

Text S2. P could be explained, first seen at line 85 (k*B)

We agree and have added an explanation in the text (Text S4 in the supplement)

Still this comparison to the tropospheric sink in Table 4 is not straight forward, the stratospheric sink also has an influence. You only need to adjust for the fraction of methane that does not return to the troposphere from the stratosphere, therefore the effect is significantly smaller than the sink itself. The Cl in the stratosphere is fairly similar in all simulations except for the SimNoCl and SimTaki. This could be discussed a bit more around line 271.

We have added a discussion regarding the stratospheric influence in Sect 3.4.

Lines 290-291. How is it estimated? "We can estimate that each percent increase in how much CH_4 is oxidized by Cl leads to an additional 0.53 ‰ increase in $\delta^{13}C(CH_4)$, ..." Linear fit to Total oxidation in Table 4 and Signature (Source adjustment) in Table 5?

We provide more information on linear fitting in the revised manuscript, in Sect. 3.3.2 and 3.3.3. Also, we use the Cl mean tropospheric concentration as the X-variable rather than the CH_4 oxidation by Cl.

Lines 294-297. The contribution from STE is estimated as 0.3 ‰, a small clarification could be made that the contribution is only from Cl, not the full contribution from stratospheric intrusions. "Intrusions of stratospheric air are therefore responsible of an enrichment at the surface stations of 0.30 ± 0.01 ‰ (depending on the latitude) after 21 years of simulation, larger than the value of Wang et al. (2002) inferred between 1970 and 1992 (0.23 ‰)." Some discussion could be added for the comparison to Wang et al result. Possible reasons for the discrepancy, different years etc. Also, the difference between SimNoCl and SimNoTropo is 0.36 (Table 5), but the value reported here 0.30 ‰, is from Fig. 2, which is not the steady state value, why is that used instead of a steady state value?

Using the $\delta^{13}C(CH_4)$ bias between FWD-NoCl and FWD-NoTropo, we provide an estimate of the influence of stratospheric Cl between 1998 and 2018. We also compare this estimate to the source signature adjustment. We note that both values are very similar.

We removed the steady state estimate because, as the reviewer mentioned before, it would be more appropriate to simulate at least 70 years with constant meteorology, fluxes and source signatures in order to have a proper estimate of this steady state value. This is not exactly the purpose of this study.

Text S2. Lines 93-96. Is it reasonable to assume delta_s equal to delta_a? Is it then also assumed that the isotopic fractionation due to the atmospheric sinks are negligible, even though the idea is to estimate the effect of chlorine on the mean atmospheric isotopic signal? Seems like this assumption going from eq(11) to eq(12) needs to be justified more thoroughly.

We do not assume that the isotopic fractionation due to the atmospheric sinks is negligible. We use the fact that the numerical value of ε, representing the isotopic fractionation, is much smaller than 1 to approximate the value of $δ_a$ by using Taylor expansion. At the end, we have $δ_a$ which is equal to $δ_s$ _MINUS_ ε. We hope that our explanation in the revised manuscript is clearer. Also, in the revised manuscript, we do not neglect the last part of the Eq. 12, resulting in a more complex, albeit more precise, relationship.

Lines 310-328. In the text related to Figure 3 in section 3.4 the reader could be reminded why the SimSherwen has an opposite bias compared to the others. It is also interesting that the SimNoTropo and SimINCA are so similar, this could also be discussed, the tropospheric Cl in SimINCA seems to have a small effect on the $δ^{13}C$. While SimNoCl seems to have a significant effect on the $δ^{13}C$ amplitude in the northern hemisphere. It is easy to understand that the differences in the bias for methane is small, but to also see small differences in the $δ^{13}C$ is a bit more surprising.

We agree with this comment. More discussion has been added in Sect. 3.2.

The discussion in section 3.5 on vertical profiles.
The number of profiles in the SH is very low, three observations in tropical latitudes, and one on mid latitudes. The validation of the SimREF is therefore not very convincing, at least for SH. In the NH there are more observations but averaging all profiles from tropical to Arctic soundings into one for the whole hemisphere is probably not good. Already the tropopause height is quite different but also the stratospheric polar vortex might have influenced the Arctic soundings. It is, however, difficult to know the reason for the observed discrepancy without seeing the individual profiles. Now the simulations were only sampled when there was a sounding. To make a more thorough analysis of the differences between the simulations the full fields should also be used. Furthermore, some discussion should be added on the $δ^{13}C$ profile.

We reshaped the analysis of AirCore profiles according to this relevant comment. Four regions are now analyzed : northern high-latitudes (Arctic), northern mid-latitudes in Europe, northern mid-latitudes in the USA and Southern Hemisphere. In addition, optimized mole fractions (after inversions) are compared to observed profiles, reducing the tropospheric bias in CH_4 mole fractions due to a poor estimation of prior CH_4 fluxes. The comparison is now more valuable, although it confirms that Cl is very likely not responsible for model-observation discrepancies at and above the tropopause. We think that comparing the full fields would not change the main picture drawn with Aircores.

We have added a section (Sect. 3.7) discussing the $δ^{13}C$ profiles with the observational data from Rockmann et al. (2011).

Line 343 "The mean bias relative to SimREF is given for all simulations and observations in Table 6." Are there any values given for observations; I find only simulations?

The mean bias is now calculated as a model-observation squared difference.

Line 343-344: "A change in the Cl field (and keeping it realistic) induces a maximum mean bias of 51 ppb in the stratosphere (SimNoCl)." I don't understand the meaning of this statement. It is the difference between a realistic Cl distribution and no Cl. Text S3.

This statement has been removed as the results, the methodology and therefore the discussion have been changed.

It is unclear what the TCCON analysis adds to the paper, especially as nothing is mentioned in the paper about the results, results are only presented in the supplementary. It is not clear which bias is presented in Fig. S5 colored dots (surface observations compared to SimNoCl or SimREF). Also, for XCH_4 it could be better to compare the simulations without filtering the data only for cases with observations. I understand that the point is to get an idea of differences in areas/times with data, in case the data would be assimilated, but without the assimilations it is not especially useful. It is somewhat interesting that the bias between SimNoCl and SimREF is latitude dependent. Probably a combination of Cl distribution and atmospheric transport but based on this analysis it remains unclear. It would perhaps make more sense to make a more rigorous analysis in another paper.

We agree with this comment and removed the GOSAT analysis. It would indeed require a more comprehensive and detailed analysis in another paper.

Lines 377-378 "...the change in the Cl field.." This conclusion should be reworded, unclear what is meant by "the change".

It has been modified.

Lines 384-385 This conclusion may need to be reworded once the previous comments have been considered, the result is not from an actual inversion. "In an inversion, this additional percent of contribution would reduce the inferred globally-averaged isotopic signature by 0.53 ‰."

This sentence has been removed since the methodology has been modified.

Lines 385-386. The authors probably mean only the contribution from Cl in the stratosphere, rather than the full impact of stratospheric intrusions. The given value is not from a steady state situation, how/why is this value chosen. The driver data ended?

We agree with this comment and the sentence has been modified. Additional information has also been provided.

Lines 388-390. This conclusion should be re-worded. This is true for the specific changes made in this study, not in general. Some other change in Cl could result in a change in $\delta^{13}C(CH_4)$ outside the 10-20 range. "CH4 seasonal cycles are only slightly influenced by a modification of the Cl sink (1-2 % change in the seasonal cycle amplitude). Changing the Cl field can nevertheless modify the amplitudes of $\delta^{13}C(CH_4)$
seasonal cycle by up to 10-20 %, depending on the latitude"

It has been modified.

The conclusions regarding the vertical profiles (Line 390-) may need to be revised once the discussion is updated. The comparison using hemispherical averages is likely not representative due to the large span of latitudes that are averaged.

Following the modifications of the Section 3.5 about AirCore profiles, this sentence has been modified.

Specific/presentation comments

All specific comments from reviewer 1 provided in the annotated pdf have been taken into account in the revised manuscript.

Some of CI fields are referred to in the manuscript as "realistic" – I strongly discourage that, as it creates impression that the regarded fields were (in)directly compared to CI observations (they were not, although indirect estimates exist). If they were, would there be the need to test five different distributions?

We agree with this comment. We removed the "realistic" mention throughout the manuscript and we no longer distinguish the tested fields.

3,32,41,etc. just use "composition" instead of "signal" (see the definition of the latter in the dictionary)

It has been modified.

5 there is a lot of processes which may fractionate whatever elements in whatever phases, so you have to be specific here, e.g. use "sink kinetics is $^{13}C/^{12}C$ fractionating"

It has been modified.

22-23 how large is "slight imbalance"?

An estimate (~ 20 $TgCH_4.yr^{-1}$) has been added.

34-35 this definition is wrong, δ notation always uses ATOMIC ratios, not molar ones – e.g. try to use your definition with isoprene (5 carbon atoms, most of isotopologues are singly substituted)

We agree and it has been modified.

36-37 there exists the (V-)PDB belemnite-based $^{13}C/^{12}C$ standard isotope ratio, however there is no standard ratio of PDB known to me

We agree and it has been modified.

40 overlaps → overlap

It has been modified.

43 "sinks are also fractionating" – in addition to which process? Emissions introduce molecules of with various isotope ratios, but this is not a fractionation process. See also comment to l. 5

We agree and it has been modified.

71 level of detail

It has been modified.

83-84 you can't claim that/reference the study that is not peer-reviewed yet

The study has just been accepted after a peer-review process with minor corrections.

86 do not use "modelling" in this context (modelling is an overall process of creating and applying models, what you refer "reproducing X and Y in the model" or similar)

It has been modified.

88 use "through the prism", that'll bear physical sense

It has been modified.

95, 98 do not use "dedicate" (you can dedicate a poem to CH4 and Cl, however). Model levels are located in stratosphere and above

Although we agree with the modification of the sentence about the model levels, "dedicate" has a meaning that corresponds exactly to what we want to convey here. See https://dictionary.cambridge.org/fr/dictionnaire/anglais/dedicated (definition : used only for one particular purpose or job)

108-109 do prescribed species have a diurnal cycle in the model? It is relevant for Tdependent reactions and KIEs, e.g., average OH concentration may be times lower than that at midday, so most of the sink occurs at higher air temperatures in the low troposphere.

Concentrations of prescribed species are daily averages so they do not have diurnal cycles. State-of-the art inversion studies mentioned in the paper only use daily or monthly averages of concentrations. Prescribing hourly averages would require much more storing capacity and I/O performance and is so far not in the scheduled developments to our knowledge.

149 irrelevant statement ("… was not mandatory")

Cl-Taki has a large influence on top-down estimates in comparison with using other Cl fields. The reader should not believe that all inversions performed as part of the Global Methane Budget used the Cl-Taki field. This sentence has been partly modified.

Figure 1 please use the same colour scale for both upper and lower panel

It has been modified.

161 exhibits → exhibit

It has been modified.

169-170 vague statement – how may your wish influence the model so that it infers a good model-observation agreement? Most comprehensive studies by no means guarantee delivering most realistic results

We agree with this comment. This sentence has been removed.

208-209 the second sentence repeats the message of the first one, remove

We agree and it has been modified.

215 to what estimates "our own estimates" refers to? Table 4 Cl concentrations are implied in columns 3 and 6?

It refers to our estimates obtained with LMDz-INCA. We modified the sentence.

Line 139. half lower than the mean tropospheric >> half of the mean

It has been modified.

Table 2. The abbreviation VPDB is not explained

We apologize for this mistake. It stands for Vienna - Pee Dee Belemnite but we only mentioned Pee Dee Belemnite (PDB) in the introduction. It has been modified.

Lines 221-223 unclear which value is meant "The tropospheric value from Hossaini et al. (2016), used in recent studies (Saunois et al., 2020; McNorton et al., 2018), is also slightly above that of ClSherwen (Table 4: 1.4 times higher) but well above that of Cl-Wang and Cl-INCA (4 and 8.5 times higher)."

It has been modified.

Table 4 third column Conc. Is not explained in the caption (average Cl conc. ?)

It has been modified.

Line 369. Cl configuration >> Cl distribution

It has been modified.

How do Cl concentrations matter for simulating CH$_4$, δ^{13}C(CH$_4$) and estimating CH$_4$ budget through atmospheric inversions ?

Joël Thanwerdas[1,*], Marielle Saunois[1], Isabelle Pison[1], Didier Hauglustaine[1], Antoine Berchet[1], Bianca Baier[2,3], Colm Sweeney[3], and Philippe Bousquet[1]

[1]Laboratoire des Sciences du Climat et de l'Environnement, LSCE-IPSL (CEA-CNRS-UVSQ), Université Paris-Saclay 91191 Gif-sur-Yvette, France.
[2]Cooperative Institute for Research in Environmental Sciences (CIRES), University of Colorado-Boulder, Boulder, CO, USA 80305.
[3]NOAA Earth System Research Laboratory Global Monitoring Division, Boulder, CO, USA 80305.

Correspondence: J. Thanwerdas (joel.thanwerdas@lsce.ipsl.fr)

Abstract. Atmospheric methane (CH$_4$) concentrations have been rising since 2007 ~~, resulting from~~ due to an imbalance between CH$_4$ sources and sinks. The CH$_4$ budget is generally estimated through top-down approaches using chemistry-transport models (CTMs) and CH$_4$ observations as constraints. The atmospheric isotopic CH$_4$ ~~signal~~composition, δ^{13}C(CH$_4$), can also provide additional constraints and helps to discriminate between emission categories. Nevertheless, to be able to use the information contained in these observations, the models must correctly account for processes influencing δ^{13}C(CH$_4$). The oxidation by chlorine (Cl) likely contributes less than 5 % to the total oxidation of atmospheric CH$_4$. However, the ~~Cl sink is highly fractionating~~large kinetic isotope effect of the Cl sink kinetics produces a large fractionation of ^{13}C compared with ^{12}C in atmospheric methane, and thus strongly influences δ^{13}C(CH$_4$). ~~As inversion studies~~When integrating the Cl sink in their setup to constrain the CH$_4$ budget, which is not yet standard, atmospheric inversion do not prescribe the same Cl fields~~to constrain budget, it can lead~~, therefore leading to discrepancies between ~~flux~~ estimates. To quantify the influence of the Cl concentrations on CH$_4$, δ^{13}C(CH$_4$) and CH$_4$ budget estimates, we perform multiple sensitivity simulations using ~~three Cl fieldswith concentrations that are realistic with regard to recent literature and one Cl field with concentrations that are very likely to be overestimated~~four different Cl fields. We also test removing the tropospheric and the entire Cl sink~~in other sensitivity simulations~~. We find that the ~~realistic~~Cl fields tested here are responsible for between 0.3~~% and 1.8 ~~% and 8.5 % of the total chemical CH$_4$ sink in the troposphere and between 1.0~~% and 1.2 ~~% and 1.6 % in the stratosphere. Prescribing these different Cl amounts in ~~surface-based~~atmospheric inversions can lead to differences of up to 53.8 TgCH$_4$.yr^{-1} in global CH$_4$ ~~source adjustments~~emissions and of up to ~~12.3 . We also find that~~4.7 ‰ in the globally-averaged isotopic signature of the total CH$_4$ ~~sources inferred by a surface-based inversion assimilating observations would decrease by 0.53~~source (δ^{13}C(CH$_4$)$_{\text{source}}$). More specifically, each increase by 1000 molec.cm^{-3} in the mean tropospheric Cl concentration would result in an adjustment by +11.7 TgCH$_4$.yr^{-1} for global CH$_4$ emissions and -1.0 ‰ for ~~each additional percent of contribution from the tropospheric Cl sink to the total sink. Finally, our study shows that~~ the globally-averaged δ^{13}C(CH$_4$)$_{\text{source}}$. Our study also shows that if the CH$_4$ seasonal cycle amplitude is only modified by less than 1-2~~% but~~ %, the δ^{13}C(CH$_4$) seasonal cycle amplitude can be significantly modified by up to 10-20 %, depending on the latitude. In an atmospheric inversion performed with isotopic

constraints, this influence can result in significant differences in the posterior source mixture. For example, the contribution
25 from wetlands emissions to total emissions can be modified by about 0.8 % to adjust the globally-averaged $\delta^{13}C(CH_4)_{source}$, corresponding to a 15 $TgCH_4.yr^{-1}$ change. Finally, tested Cl concentrations have a large influence on the simulated $\delta^{13}C(CH_4)$ vertical profiles above 30 km, albeit this influence is small below this altitude, and they have a very small influence on the simulated CH_4 vertical profiles. Overall, our model captures well the observed CH_4 and $\delta^{13}C(CH_4)$ vertical profiles, especially in the troposphere and it is difficult to prefer one Cl field over another based uniquely on the available observations of vertical
30 profiles.

1 Introduction

Methane (CH_4) is a very important species for both atmospheric chemistry and climate. Its atmospheric mole fractions have reached an average of ~~1879~~1896 ppb at the surface in ~~2020 (Dlugokencky, 2021)~~2021 (Dlugokencky, 2022), almost three times higher than pre-industrial mole fractions (Etheridge et al., 1998). After a plateau between 1999 and 2006, CH_4 mole
35 fractions resumed their increase in 2007 without showing any sign of stabilization since then. The increase has even reached an unprecedented value of +~~15.9~~16.9 ppb for the year ~~2020.~~2021 (Dlugokencky, 2022). The accumulation of CH_4 ($\sim$ 8 $ppb.yr^{-1}$ on average since 2007) in the atmosphere is the result of ~~a slight imbalance~~ an imbalance of about 20 $TgCH_4.yr^{-1}$ (Saunois et al., 2020) between sources that release CH_4 into the atmosphere and sinks that remove it. Sinks are mostly due to oxidation reactions in the atmosphere ~~. Three radicals react with~~ between CH_4 ~~in the atmosphere~~ and three radicals : hydroxyl
40 (OH), atomic oxygen (O^1D), and chlorine (Cl). These chemical reactions account for about 93 % of the total CH_4 sink, with the remainder being removed by methanotrophic bacteria in the soil (Saunois et al., 2020). On the other hand, CH_4 sources are varied and result from radically different processes (biogenic, thermogenic and pyrogenic).

Estimating global CH_4 sources with precision is a mandatory step, yet challenging, towards implementing efficient mitigation policies. Top-down atmospheric inversions are known to be efficient approaches to estimate CH_4 sources at different scales and
45 have become increasingly relevant over the years as observational networks have developed (Houweling et al., 2017, and references therein). However, inversions that assimilate only total CH_4 observations can only rely on variations in seasonal cycles to differentiate co-located emissions. To better separate these sources, assimilating observations of the $^{13}C:^{12}C$ atmospheric isotope ~~signal~~ composition of CH_4, denoted by $\delta^{13}C(CH_4)$, can be relevant. This value is based on the ratio between the isotopologue $^{12}CH_4$, which represents about 99 % of the CH_4 in the atmosphere (Stolper et al., 2014) and its counterpart $^{13}CH_4$.
50 $\delta^{13}C(CH_4)$ is commonly defined using a deviation of the sample ~~mole~~ atomic isotopic ratio relative to a specific standard ratio :

$$\delta^{13}C(CH_4) = \frac{R}{R_{std}} - 1 = \frac{[^{13}CH_4]/[^{12}CH_4]}{R_{std}} - 1 \qquad (1)$$

~~and denote the and mole fractions, respectively~~R represents the abundance of ^{13}C relative to ^{12}C in all CH_4 molecules. R_{std} = 0.0112372 is here the standard ratio of Vienna - Pee Dee Belemnite (~~PDB~~VPDB) (Craig, 1957).

55   CH$_4$ sources exhibit specific isotopic signatures that are mainly controlled by the process involved ~~in the production of~~ CH$_4$. Broadly summarized, most biogenic sources have an isotopic signature between -65 and -55 ‰, thermogenic sources between -50 and -30 ‰ and pyrogenic sources between -25 ‰ and -15 ‰ (Sherwood et al., 2017), although the ~~distributions~~ full distributions of these signatures are very large ~~and overlaps exist between the extreme~~ with overlapping values. The post-2007 CH$_4$ increase is notably associated with a decrease in the atmospheric isotopic ~~signal~~ composition δ^{13}C(CH$_4$) (Nisbet et al.,

60   2019) ~~and these isotopic variations~~ that could help to better explain ~~this renewed growth and~~ the renewed CH$_4$ growth and, more specifically, the contribution from the different CH$_4$ sources to it.

    The sinks ~~are also fractionating,~~ also have an influence on δ^{13}C(CH$_4$) as they remove ^{12}CH$_4$ faster than ^{13}CH$_4$. This effect, called the Kinetic Isotope Effect (KIE) or isotopic fractionation, is quantified using the ratio of the reaction rate constants X + ^{12}CH$_4$ and X + ^{13}CH$_4$, with X the species of interest (X = OH, O(^{1}D) or Cl). KIE$_X$ = k$_{12}^X$/k$_{13}^X$ with k$_{12}^X$ and k$_{13}^X$ being the

65   oxidation reaction rate constants. As a result, δ^{13}C(CH$_4$) depends on both sources and sinks, ~~as~~ like total CH$_4$, but also on the isotopic fractionation and the ~~sources isotopic signatures~~ isotopic signatures of the sources.

    Among all CH$_4$ sinks, the Cl sink accounts for a small part of the total CH$_4$ oxidation. Following the discovery of the dramatic impact of Cl on ozone in the stratosphere, many studies have ~~first~~ focused on the impact of stratospheric Cl on CH$_4$ and δ^{13}C(CH$_4$) using box or 2-D models (e.g., Röckmann et al., 2004; McCarthy et al., 2003; Wang et al., 2002; McCarthy

70   et al., 2001; Saueressig et al., 2001; Gupta et al., 1996; Müller et al., 1996). McCarthy et al. (2003) estimated that Cl was responsible for 20-35 % of CH$_4$ removal in the stratosphere. Saunois et al. (2020) suggested a range of values for the total stratospheric sink between 12 and 37 TgCH$_4$.yr^{-1}, leading to a plausible stratospheric Cl sink of 2-13 TgCH$_4$.yr^{-1}, or about only 0.4-2.4 % of the total CH$_4$ oxidation in the atmosphere. Although this contribution is very small, the Cl sink is particularly important because of its large fractionation effect (KIE = 1.066 for the Cl sink against 1.0039 for the OH sink, see Sect. 2.1).

75   The aforementioned studies showed that stratospheric Cl has a strong impact on δ^{13}C(CH$_4$) not only in the stratosphere but also ~~at~~ closer to the surface. In particular, Wang et al. (2002) estimated that stratospheric Cl was responsible for a δ^{13}C(CH$_4$) enhancement of 0.23 ‰ at the surface between 1970 and 1992 due to stratosphere-troposphere exchanges (STE).

    In the troposphere, the Cl sink likely accounts for less than 5 % of CH$_4$ oxidation (Wang et al., 2019, 2021; Hossaini et al., 2016; Sherwen et al., 2016b; Gromov et al., 2018; Allan et al., 2007). Several studies have estimated Cl concentrations in the

80   troposphere and in the Marine Boundary Layer (MBL) and discussed the Cl sink. Allan et al. (2007) estimated the Cl sink in the troposphere to be 25 TgCH$_4$.yr^{-1}, representing about 5 % of the total CH$_4$ chemical sink. More recently, Hossaini et al. (2016), Sherwen et al. (2016b), Wang et al. (2019) and Wang et al. (2021) have made important developments in tropospheric chemistry modeling (see Sect 2.2) and obtained oxidation contributions of 2.6 %, 2 %, 1 % and 0.8 % respectively with mean tropospheric Cl concentrations between 620 and 1300 molec.cm^{-3}. However, Gromov et al. (2018) concluded that variations

85   in Cl concentrations above 900 molec.cm^{-3} in the extratropical part of the Southern Hemisphere are very unlikely ; thus suggesting that the high estimates from Allan et al. (2007) and Hossaini et al. (2016) are likely overestimated. ~~These variations in~~ This estimated range of oxidation contributions may appear small but Strode et al. (2020) recently showed a high sensitivity of the tropospheric δ^{13}C(CH$_4$) distribution to variation in Cl fields by testing, among others, those of Allan et al. (2007), Sherwen et al. (2016b) and Hossaini et al. (2016), indicating that each percent increase in how much CH$_4$ is oxidized by Cl

90   leads to a 0.5 ‰ increase in $\delta^{13}C(CH_4)$, therefore larger than the global downward shift observed since 2007 (Nisbet et al., 2019).

Forward and inverse 3-D modeling studies focusing on CH_4 and $\delta^{13}C(CH_4)$ consider the Cl sink at different level of ~~details~~detail. Most studies consider only the Cl sink in the stratosphere (e.g., Fujita et al., 2020; Rigby et al., 2012; Monteil et al., 2011; Fletcher et al., 2004), and a very few account for tropospheric Cl only (e.g., Thompson et al., 2018). In single-box

95   models, sinks are combined and an overall fractionation coefficient is used (e.g., Schaefer et al., 2016; Schwietzke et al., 2016). In recent studies, Cl is often prescribed in both the troposphere and stratosphere (e.g., McNorton et al., 2018; Rice et al., 2016; Warwick et al., 2016; Neef et al., 2010), although most studies use the Cl ~~configuration~~ distribution suggested by Allan et al. (2007), which is likely to be overestimated as mentioned above.

In the atmospheric inversions performed with the LMDz-SACS chemistry-transport model (Locatelli et al., 2015; Pison

100   et al., 2009), the Cl sink was omitted so far, even in the stratosphere (Saunois et al., 2020; Locatelli et al., 2015; Pison et al., 2009; Bousquet et al., 2006). For these studies assimilating only total CH_4 observations, the impact of the Cl sink on the estimated CH_4 emissions was considered negligible. However, the number and quality of isotopic observations have considerably increased since the 2000s, and developments of the CIF-LMDz-SACS inversion system to use the isotopic constraint have been made (Thanwerdas et al., 2021). Joint assimilation (CH_4 and $\delta^{13}C(CH_4)$) is proving to be relevant and necessary in order

105   to reconcile the estimated CH_4 budgets with the atmospheric isotope ~~signal~~composition. Considering the large impact of the Cl sink on $\delta^{13}C(CH_4)$, it is necessary to include and evaluate the Cl sink and its impact on the simulation of CH_4 ~~modeling process~~and $\delta^{13}C(CH_4)$ with our model.

Here, we detail the influence of tropospheric and stratospheric Cl on the modeling of CH_4 and $\delta^{13}C(CH_4)$ in LMDz-SACS by using several Cl fields. ~~Ultimate goal being to use the isotopic signal~~ The ultimate aim is to assimilate the isotopic

110   composition observations to perform multi-constraint inversions with the LMDz-SACS model~~, results are analyzed throughout the study under~~. Therefore the developments performed and the results obtained are analyzed through the prism of atmospheric inversion. In ~~the first part~~Sect. 2, we present the characteristics of the available Cl fields, model inputs and observations used for evaluation. ~~Then~~In Sect. 3, we analyze the influence of the different Cl fields on CH_4 and $\delta^{13}C(CH_4)$ at the surface, on global CH_4 flux and $\delta^{13}C(CH_4)$ source signature adjustment obtained with inversion methods and on the CH_4 ~~vertical profile~~and

115   $\delta^{13}C(CH_4)$ vertical profiles.

2   Methods

2.1   The chemistry-transport model (CTM)

The general circulation model (GCM) LMDz is the atmospheric component of the coupled model of the Institut Pierre-Simon Laplace (IPSL-CM) developed at the Laboratoire de Météorologie Dynamique (LMD) (Hourdin et al., 2006). The version

120   of LMDz used here is an "offline" version dedicated to the inversion framework created by Chevallier et al. (2005): the precalculated meteorological fields provided by the online version of LMDz are given as input to the model, which considerably reduces the computation time. The model is built at a horizontal resolution of 3.8° × 1.9° (96 grid cells in longitude and latitude)

with 39 hybrid sigma pressure levels reaching an altitude of about 75 km. About 20 levels are ~~dedicated to~~ located in the stratosphere and ~~the mesosphere~~above. The time step of the model is 30 min and the output values have a resolution of 3 hours.

125   Horizontal winds have been nudged towards the ECMWF meteorological analyses (ERA-Interim) in the online version of the model. Vertical diffusion is parameterised by a local approach of Louis (1979), and deep convection processes are parameterised by the scheme of Tiedtke (1989). The offline model LMDz, coupled with the Simplified Atmospheric Chemistry System (SACS) module (Pison et al., 2009), was previously used to simulate atmospheric mole fractions of trace gases such as CH_4, carbon monoxide (CO), methyl chloroform (MCF), formaldehyde (CH_2O) or hydrogen (H_2). This system has been recently

130   converted into a chemistry parsing system (Thanwerdas et al., 2021). It follows the principle of the chemical parsing system of the regional model CHIMERE (Mailler et al., 2017; Menut et al., 2013) and allows the user to prescribe the set of chemical reactions to consider. Consequently, it generalizes the SACS module to any set of possible reactions. The concentration fields of the different species are either prescribed or simulated. Prescribed species (here OH, O(^{1}D) and Cl) are not transported in LMDz, and their mole fractions are not updated by chemical production or destruction. These species are only used to

135   calculate reaction rates and update the mole fractions of transported species at each iteration of the model. In this study, the $^{12}CH_4$ and $^{13}CH_4$ isotopologues are simulated as separate tracers and CH_4 mole fractions are defined as ~~a sum of~~the sum of the mole fractions of the two isotopologues. Oxidation by Cl + CH_4 was added to complete the chemical removal of CH_4, which only considered OH + CH_4 and O(^{1}D) + CH_4 reactions in the original SACS chemical scheme. The photolysis of CH_4 is not included in SACS as it is considered negligible. None of the inversion studies mentioned above, in particular those of

140   Saunois et al. (2020), accounted for this sink.

Reactions between $^{12}CH_4$ and OH, O(^{1}D) and Cl are represented by the chemical equations below, and similar equations apply to $^{13}CH_4$:

$$^{12}CH_4 + OH \quad \rightarrow \quad ^{12}CH_3 + H_2O \tag{R1}$$

$$^{12}CH_4 + Cl \quad \rightarrow \quad ^{12}CH_3 + HCl \tag{R2}$$

145   $$^{12}CH_4 + O(^1D) \quad \rightarrow \quad ^{12}CH_3 + OH \tag{R3}$$

$$^{12}CH_4 + O(^1D) \quad \rightarrow \quad H_2 + ^{12}CH_2O \tag{R4}$$

Three-dimensional and time-dependent oxidant concentration fields (OH, O(^{1}D) and Cl) were simulated by the GCM LMDz coupled to the INteraction with Chemistry and Aerosols (INCA) model (Hauglustaine et al., 2021; Folberth et al., 2006; Hauglustaine et al., 2004). Seventeen ozone-depleting substances ~~consisted~~ consisting of CFCs (CFC-12, CFC-11, CFC-113),

150   three HCFCs (HCFC-22, HCFC-141b, HCFC-142b), two halons (Halon-1211, Halon-1301), methyl chloroform (CH_3CCl_3 or MCF), carbon tetrachloride (CCl_4), methylchloride (CH_3Cl), methylene chloride (CH_2Cl_2), chloroform ($CHCl_3$), methyl bromide (CH_3Br) and HFC-134a, and their associated photochemical reactions, were included in the INCA chemical scheme to produce Cl radicals ~~(?)~~(Terrenoire et al., 2022). In the LMDz-INCA simulations, surface concentrations of these long-lived Cl ~~source species~~precursors were prescribed based on historical data sets prepared by Meinshausen et al. (2017). The model

155   was run for the 1850-2018 period (Hauglustaine et al., 2021).

Table 1. Reaction rate constants and KIEs of CH$_4$ chemical sinks. The reaction rate constants are taken from Burkholder et al. (2015).

Oxidant	KIE	Reference	Reaction rate constant (cm^3 molec^{-1} s^{-1})
OH	1.0039	Saueressig et al. (2001)	$2.45 \times 10^{-12} \cdot$ exp(-1775/T)
Cl	$1.043 \cdot$ exp(6.455/T)	Saueressig et al. (1995)	$7.1 \times 10^{-12} \cdot$ exp(-1280/T)
O(^{1}D) - R3	1.013	Saueressig et al. (2001)	1.125×10^{-10}
O(^{1}D) - R4	1.013	Saueressig et al. (2001)	3.75×10^{-11}

All reaction rate constants and associated values used in LMDz-SACS are given in Table 1. The reaction rate constants with ^{13}CH$_4$ are modified based on the definition of the ~~fractionation coefficient (KIE)~~KIE. Few studies have evaluated the KIEs associated with CH$_4$ chemical sinks (particularly for O(^{1}D) and Cl) over a wide range of temperatures and thus large uncertainties remain. For CH$_4$ + OH, we adopted the value of Saueressig et al. (2001) as they indicate that this data is of considerably higher experimental precision and reproducibility than previous studies, in particular Cantrell et al. (1990), which suggested a value of 1.0054.

2.2 Description of Cl fields

Four fields of Cl are ~~used~~ compared in this study. ~~The first field was simulated by the~~ Two fields were generously provided by the respective authors of Sherwen et al. (2016b) and Wang et al. (2021). They will be referred to as the Cl-Sherwen and Cl-Wang fields. Sherwen et al. (2016b) obtained the associated Cl field using version 10 of the GEOS-Chem CTM (https://geos-chem.seas.harvard.edu/, version 10) running at a 4° × 5° spatial resolution. Previously, Sherwen et al. (2016a) extended the stratospheric chlorine scheme to the troposphere. Sherwen et al. (2016b) improved the coupling of halogens (Br, Cl, I) chemistry and further updated the chlorine chemistry scheme. Subsequently, Wang et al. (2019) focused principally on the modelling of tropospheric reactive chlorine by developing the treatment of sea salt aerosol (SSA) chloride and chlorine gases, as well as SSA acid displacement thermodynamics, starting from version 11-02d of GEOS-Chem. Chloride mobilisation from SSA by acid displacement of HCl represents a significant source of reactive chlorine in the troposphere. The authors also mentioned a better accounting of other chlorine sources (combustion, organochlorines, transport from the stratosphere, anthropogenic HCl) compared to previous versions. Wang et al. (2020, 2021) made some additional developments that appear to have a relatively small impact on the atomic Cl spatial distribution and mean concentration in the troposphere. They did not include continental anthropogenic emissions of inorganic Cl (coal combustion, waste incineration, and industrial activities) because existing estimates are likely outdated and carry too high uncertainties. Consequently, the Cl concentrations from Wang et al. (2021) may be underestimated over regions where relatively high anthropogenic chlorine sources have been reported (e.g. China).

Another field was simulated by the LMDz-INCA ~~model, as mentioned above. More details on the modeling of this field are available in the supplement~~model, as mentioned in Sect. 2.1. This field will be referred to as the Cl-INCA field. At ~~this stage~~present, simulations performed with the LMDz-INCA model do not fully represent the chemical interactions between
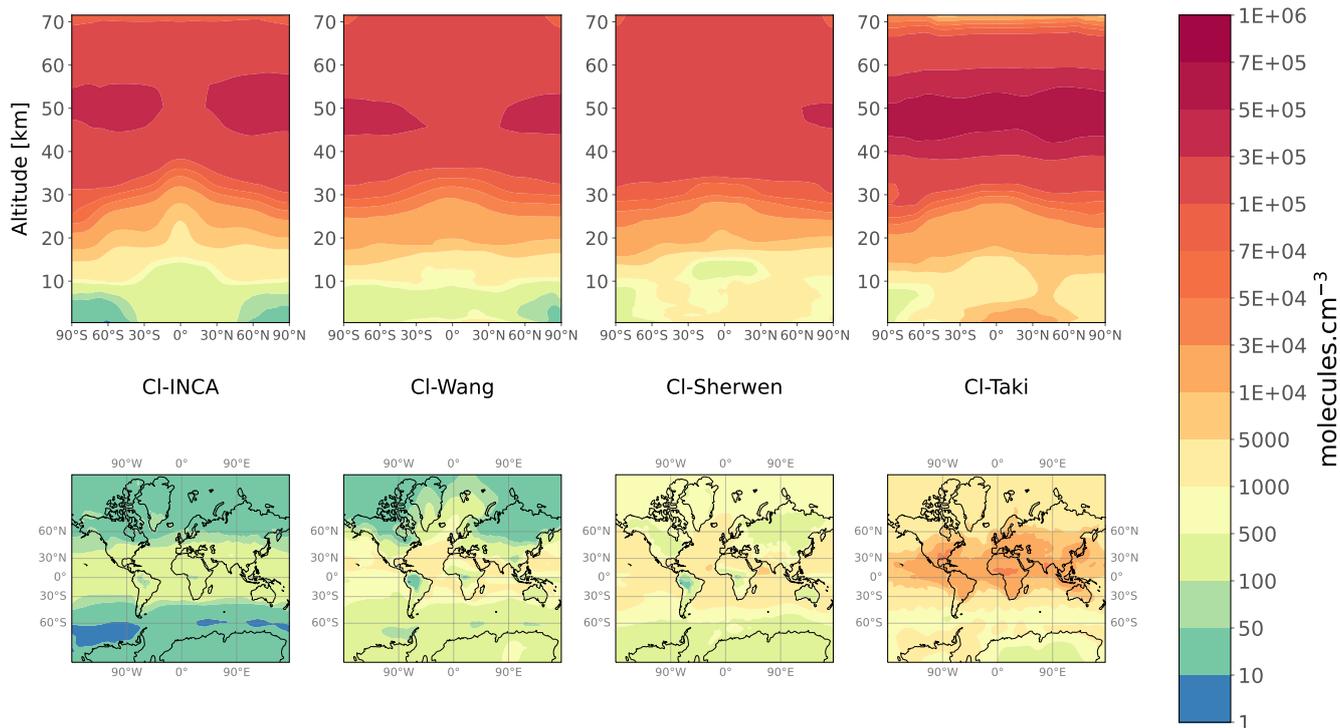
Figure 1. Annual mean meridional cross-section (upper panels) and tropospheric Cl concentrations (lower panels) for the four 3-D fields Cl-INCA, Cl-Wang, Cl-Sherwen and Cl-Taki.

Cl and other species in the troposphere. ~~Developments~~ In particular, developments are currently being made to improve ~~these interactions~~ the treatment of SSA and chloride mobilisation from SSA. Cl-INCA did not benefit from such enhancements, resulting in significant discrepancies compared to Cl-Wang and Cl-Sherwen. The mean tropospheric Cl concentration (330 molec.cm^{-3})

185   in the Cl-INCA field is ~~therefore about half lower than the mean tropospheric value~~ about half of the tropospheric mean (630 molec.cm^{-3}) of Wang et al. (2021)~~or other studies, but~~, but is in agreement with the upper limits inferred by Gromov et al. (2018).

     ~~Two fields were simulated using the versions of the GEOS-Chem model () of Sherwen et al. (2016b) and Wang et al. (2021) (i.e., v10 and v12.9, respectively). These fields were generously provided by the respective authors of the two studies. They~~

190   ~~will be referred to as the Cl-Sherwen and Cl-Wang fields. Differences between the two fields are detailed below.~~

     The last field was simulated by version 5.7b of the CCSR/NIES/FRCGC (Center for Climate Sytem Research/National Institute for Environmental Studies/Frontier Research Center for Global Chance) atmospheric GCM (Takigawa et al., 1999). This was provided by the GCP-GMB (Global Carbon Project - Global Methane Budget) team to run the inversions used in Saunois et al. (2020), although ~~it was not mandatory. It is referred to as the Cl-Taki field.~~

195   ~~Annual mean meridional cross-section (upper panels) and tropospheric Cl concentrations (lower panels) for the four 3-D fields Cl-INCA, Cl-Wang, Cl-Sherwen and Cl-Taki.~~

In this study, we do not test the Cl fields from Hossaini et al. (2016) and Allan et al. (2007) because we want to carry out the sensitivity analysis while keeping a realistic and up-to-date range of concentrations. Their concentrations are indeed very likely to be overestimated (Gromov et al., 2018). Although Cl concentrations in the some inversions did not prescribe it. The model did not include any treatment of SSA and chloride mobilisation from SSA. More generally, it did not include any representation of tropospheric reactive chlorine chemistry. We could not have access to additional information regarding this field. It is referred to as the Cl-Taki field are also very large, to our knowledge, oxidation resulting from the prescription of this field has not been studied before. We therefore choose to include it here in order to quantify the associated sink and to illustrate the influence of such concentrations on and field.

The four fields are shown in Fig. 1. We use the lapse rate (2 K/km) definition from the World Meteorological Organization (WMO) and the meteorological fields from the online LMDz model to define the tropopause. Global mean tropospheric Cl concentrations range between from 330 (Cl-INCA) and to 4730 (Cl-Taki) molec.cm^{-3}. The latitudinal distributions of tropospheric concentrations are similar, although Cl-Wang, Cl-Sherwen and Cl-Taki have a greater spatial variability around their mean value than Cl-INCA, especially in the mid-latitudes (75 %, 66 % and 63 % against 36 %, respectively). Cl-Wang, Cl-Sherwen and Cl-INCA exhibits exhibit similar concentrations in the stratosphere ($1.45 \pm 0.07 \times 10^5$ molec.cm^{-3}). The increase in concentrations with altitude between the surface and 30 km is similar between all the fields, with a 0-30 km vertical gradient of $4.4 \pm 1.0 \times 10^4$ molec.cm^{-3}. Stratospheric concentrations are however larger in Cl-Taki, reaching a mean value of 2.1×10^5 molec.cm^{-3}.

In this study, we do not test the Cl fields from Hossaini et al. (2016) and Allan et al. (2007) because the fields presented above cover a range of tropospheric and stratospheric Cl concentrations wide enough to carry out a robust analysis.

2.3 Description of simulations

The time period adopted for all simulations here is 1998-2018, long enough to capture the large equilibration time associated with δ^{13}C(CH$_4$). Mole fractions of ^{12}CH$_4$ and ^{13}CH$_4$ are simulated over the 1998-2018 period . The distributions of OH and O(^{1}D) have also been simulated with the LMDz-INCA model and are outputs of the same simulation that provided the Cl-INCA field. These OH and O(^{1}D) fields are used in all simulations performed here this period of time in multiple simulations, either forward or inverse.

Our SimREF reference simulation uses the Cl-Wang field as it is the most recent field and is taken from the most comprehensive study to date. In addition, we want our reference simulation to infer realistic and distributions with a good model-observation agreement. The fluxes and isotopic signatures of five emission categories used in this study therefore result from an atmospheric inversion First, a set of optimized fluxes and source signatures are obtained by running atmospheric variational inversions over 1998-2018 based on a joint assimilation of CH$_4$ and δ^{13}C(CH$_4$) in the CIF-LMDz-SACS system designed by Thanwerdas et al. (2021). The inversion assimilates observations introduced in Sect. 2.4. The Cl-Wang field was not available when this inversion was launched. Therefore, we instead prescribed the Cl-INCA field and scaled the tropospheric mean Cl concentration (330) to that of Wang et al. (2019) (620), very similar to that of Wang et al. (2021) (630). We acknowledge the small difference between the inversion setup and the reference scenario setup, due to small differences in Cl concentrations. However, using the

8

~~optimized fluxes and signatures together with the prescribed sinks, a model-observation agreement (Root Mean Square Error) of 3.6 ppb for~~ A variational inversion consists in performing alternate runs of the CTM's forward and adjoint codes to calculate the cost function and its gradient. A global minimum of this cost function is then sought using an adequate minimization algorithm. With our method, multiple iterations of this process are performed until a satisfactory convergence criterium is reached. At the end of the minimization process, we obtain posterior fluxes and source signatures that reduce the discrepancies between observed and simulated CH_4 and ~~0.04 for~~ $\delta^{13}C(CH_4)$ ~~is obtained on global averages, and is considered sufficient to validate the conclusions of this study. More information about the inversion is given in the supplement (Text S1).Emissions and source isotopic signatures are given in Table ??. Both vary over time and space and are prescribed as monthly fields at the horizontal resolution of the model.~~

~~The~~, compared with prior estimates. Our system typically runs a last forward simulation with optimized inputs at the end of the inversion process.

One variational inversion is run for each Cl field presented in Sect. 2.2. The Cl-Wang, Cl-Sherwen, Cl-Taki and Cl-INCA fields ~~presented in Sect. 2.2~~ are used in the ~~SimSherwen, SimTaki and SimINCA simulations~~INV-Wang, INV-Sherwen, INV-Taki and INV-INCA inversions, respectively. In Saunois et al. (2020), the majority of inversions ~~are~~ were performed without a tropospheric Cl sink; thus, we ~~tested this with the SimNoTropo simulation where~~ perform one inversion using the Cl-Wang ~~is used but with no Cl in the troposphere. Moreover~~field but without tropospheric Cl (INV-NoTropo). Finally, as LMDz-SACS completely omitted the Cl sink in previous studies, we estimate the errors generated by this omission ~~running the SimNoCl simulation, which has no Cl sink. A summary of the simulations and their characteristics is provided~~ by running a last inversion without Cl sink (INV-NoCl). More information about the variational inversion method, the inversion system used here and the setup of these inversions is provided in the supplement (Text S1). Apart from the prescribed Cl field, all these inversions share the same configuration. Consequently, for each inversion, we obtain a different set of fluxes and source signatures and the differences between them result only from the influence of Cl concentrations. These differences are analyzed in Sect. 3.3 and Sect. 3.4.

As mentioned above, the last forward simulation of a variational inversion is performed with optimized inputs. Hereinafter, INV-* outputs (simulated values) refer to the results of the last forward simulation performed with the optimized fluxes and source signatures derived from the corresponding inversion, prescribed as monthly fields at the horizontal resolution of the model. As expected, CH_4 and $\delta^{13}C(CH_4)$ simulated with the posterior fluxes and source signatures are all consistent with assimilated observations (see supplementary Fig. S1). Emissions and source isotopic signatures obtained with INV-Wang are given in Table ~~3~~2. They both vary over time and space.

A set of simple forward simulations (FWD-*) with identical prescribed fluxes and source signatures are also run to quantify the biases in CH_4 and $\delta^{13}C(CH_4)$ that arise from differences in prescribed Cl field, hence differences in atmospheric sink. The posterior fluxes and source signatures from INV-Wang are used for all FWD-* simulations because the Cl-Wang field is taken from the most comprehensive and recent study to date. A different Cl field is prescribed for each simulation, resulting in six forward simulations : FWD-Wang, FWD-Sherwen, FWD-Taki, FWD-INCA, FWD-NoTropo and FWD-NoCl. Apart from the

prescribed Cl field, all these simulations adopt the same configuration. Consequently, note that the FWD-Wang and INV-Wang inputs and outputs are identical.

To summarize :

- – INV-* outputs are consistent with observed CH$_4$ and δ^{13}C(CH$_4$) because they use optimized fluxes and source signatures derived from a variational inversion.

- – Apart from FWD-Wang, FWD-* outputs are not consistent with observed values because they all adopt the same fluxes and source signatures.

Table 2. Global CH$_4$ emissions and associated flux-weighted isotopic signatures by source category obtained with INV-Wang. Given values are averages over 1998-2018. Numbers in brackets are minimum and maximum over this period of time [min/max].

Categories	CH$_4$ emissions (TgCH$_4$.yr^{-1})	Isotopic signature (‰ - VPDB)
Biofuels-Biomass Burning (BB)	28 [23 / 44]	-21.5 [-22.2 / -21.3]
Agriculture and Waste (AGW)	221 [197 / 241]	-58.3 [-59.4 / -57.0]
Fossil Fuels and Geological sources (FFG)	124 [101 / 142]	-43.5 [-44.8 / -42.1]
Natural sources apart from wetlands (NAT)	23 [23 / 23]	-50.8 [-50.8 / -50.8]
Wetlands (WET)	192 [184 / 202]	-56.6 [-56.6 / -56.5]
Total	588 [530 / 639]	-52.6 [-53.3 / -52.0]

2.4 Observations

Different datasets of observations are either assimilated in our inversions or used to evaluate our simulations and to estimate the impact of the Cl field. These observations are of several types~~and could be assimilated in atmospheric inversions~~: surface measurements of CH$_4$ and δ^{13}C(CH$_4$)~~as well as~~, in situ vertical profiles of CH$_4$ ~~.~~and in situ vertical profiles of δ^{13}C(CH$_4$)

CH$_4$ observations measured at 79 surface stations of the Global Greenhouse Gas Reference Network (GGGRN), part of the NOAA-ESRL's Global Monitoring Laboratory (NOAA GML), ~~were used to perform the inversion~~ are assimilated in the inversions introduced in Sect. ~~??~~2.3. Reported uncertainties are generally below 5 ppb. δ^{13}C(CH$_4$) measurements provided by the Institute of Arctic and Alpine Research (INSTAAR) by analyzing air samples collected at 22 stations on an approximately weekly basis ~~were~~ are also assimilated (White et al., 2021). Reported uncertainties are generally below 0.15 ‰.

~~A total of 11 MBL sites (i.e., the site samples consist mainly of well-mixed MBL air) among those that recorded values over the 1998-2018 period were selected to sample simulated values at the time and locations of available observations.~~ The station locations and additional information can be found in the supplementary Figure S3, Tables ~~S5 and~~ S6 and S7.

~~Finally, an~~

An analysis of the impact of Cl on CH$_4$ vertical profiles is also conducted using a set of 115 AirCore profiles recovered from 11 different sites over the 2012-2018 period. A total of 80 profiles are provided by the NOAA GML aircraft programme (Baier

Table 3. Nomenclature and description of the sensitivity tests performed in this study. The INV-* simulations refer both to the variational inversion performed with the system of Thanwerdas et al. (2021) and to the final forward simulation of this inversion process with associated optimized fluxes and source signatures. For each test, the model used to simulate Cl concentrations is given. Forward sensitivity tests (FWD-*) have also been run with identical optimized fluxes and source signatures based on the INV-Wang outputs. Note that INV-Wang and FWD-Wang are identical.

~~Sensitivity~~ Inverse sensitivity test	Forward sensitivity test	Chemistry model	Field name	Modification
~~SimNoCl~~ INV-NoCl	FWD-NoCl	None	None	None
INV-NoTropo	FWD-NoTropo	GEOS-Chem v12.09 Wang et al. (2021)	Cl-Wang	No Cl in the troposphere
INV-Wang	FWD-Wang	GEOS-Chem v12.09 Wang et al. (2021)	Cl-Wang	None
~~SimINCA~~ INV-INCA	FWD-INCA	LMDz-INCA	Cl-INCA	None
INV-Sherwen	FWD-Sherwen	GEOS-Chem v10 Sherwen et al. (2016b)	Cl-Sherwen	None
INV-Taki	FWD-Taki	CCSR/NIES/FRCGC AGCM v5.7b Takigawa et al. (1999)	Cl-Taki	None

et al., 2021; Karion et al., 2010) and 35 others by the French AirCore programme (Membrive et al., 2017). The balloon-borne AirCore technique (Karion et al., 2010) allows air samples to be taken from the stratosphere (up to approximately 30 km) to the ground, upon a parachute-based descent. Figure S4 and Table S4, in the supplement, provide information about the provider, location and number of profiles collected. Reported uncertainties generally increase with altitude due to end-member mixing within the AirCore samples. They are below 2 ppb in the troposphere and can reach 10 ppb in the lower stratosphere.

We also use air samples from stratospheric balloon flights analyzed in Röckmann et al. (2011) to compare simulated vertical profiles of $\delta^{13}C(CH_4)$ to observations. Figure S5 and Table S5, in the supplement, provide information about the time, location and number of profiles collected. The samples were retrieved at four different locations from subtropical to high latitudes, above an altitude of 10 km and up to 35 km. Uncertainties are generally below 0.2 ‰.

2.5 Estimating global CH_4 flux and $\delta^{13}C(CH_4)$ source signature adjustments

Three methods are employed to quantify the influence of the Cl sink on inversions adjusting both CH_4 fluxes and isotopic signatures of sources, here denoted by $\delta^{13}C(CH_4)_{source}$. Simple descriptions of the three methods are provided here whereas comprehensive descriptions are given in the supplement (Text S1, S2 and S3).

The first approach (M1) is based on the INV-* inversions presented in Sect. 2.3 and the 3-D variational inversion system from Thanwerdas et al. (2021). Although this approach is the most robust among the three methods used here, the associated computational burden is also the largest. At present, approximately 4 months are necessary to reach a satisfactory convergence criterion with this system for a 20-year assimilation window, which is highly excessive if one must use this method every

time the influence of two Cl fields are to be compared. Here, we employ this method to show that the two other methods provide global results that are consistent with this robust approach but also to benefit from the high spatial resoluton of the CIF-LMDz-SACS system and therefore perform an analysis at smaller spatial scales. Optimized CH_4 fluxes and source signatures are directly taken from INV-* results. More information is provided in Text S1.

The second approach (M2) employs a box-model analytical inversion system assimilating both CH_4 and $\delta^{13}C(CH_4)$ observations. This system has been specifically designed for the purpose of this study. The $^{12}CH_4$ and $^{13}CH_4$ mole fractions in the troposphere are simulated with this box model, converted to CH_4 mole fractions and $\delta^{13}C(CH_4)$ values and compared to globally-averaged observations provided by the NOAA GML. An analytical non-linear method is then applied to find the optimal solution of the inversion problem. This method is extremely simple to use and very fast ($\sim$ 1 minute) but requires the input parameters of the box model (global lifetime, KIE and conversion factor between CH_4 mass and mole fractions) to be computed prior to the inversion. Here, these input parameters are derived from the forward simulations described in Sect. 2.3. More information is provided in Text S2.

The third approach (M3) is not an inversion in its strictest definition. It is only based on an analysis of the time-series of the bias in CH_4, $^{12}CH_4$ and $^{13}CH_4$ total atmospheric masses between two forward simulations (FWD-*) described in Sect. 2.3. This bias increase over time but stabilize after several decades. We derive a simple theoretical framework to predict the adjustment value that an inversion system would apply to the prior global CH_4 flux and the globally-averaged $\delta^{13}C(CH_4)_{source}$ in order to offset this bias. More information is provided in Text S3. This method is less robust than the other ones but does not require to perform an inversion. In Sect. 3.3 and Sect. 3.4, we show that M3 provides results that are very consistent with M1 and M2.

3 Results

3.1 Quantification of the Cl sink

The simulated chemical sink of CH_4 due to Cl oxidation varies depending on the prescribed Cl field. ~~We therefore obtain different sink intensities depending on the simulation.~~ Table 4 summarizes the ~~intensities of these sinks~~ multiple estimates averaged over the ~~simulation~~ 1998-2018 period in both the troposphere and stratosphere. Also included in the comparison are the tropospheric Cl sinks from Hossaini et al. (2016) and Allan et al. (2007), and the stratospheric Cl sink from Patra et al. (2011). All of them are used in many CH_4 inversions. The Cl sink used in Patra et al. (2011), which is exclusively stratospheric, is the sum of $O(^1D)$ and Cl sinks. Contributions of $O(^1D)$ and Cl sinks to the stratospheric sink were previously estimated to be 20-40 % and 20-35 %, respectively (McCarthy et al., 2003; Rice et al., 2003). Using these estimates, the Cl sink from Patra et al. (2011) should contribute between 1.3 % and 2.6 % of the total sink. Using our ~~own~~ estimates of $O(^1D)$ concentrations obtained with LMDz-INCA (see Sect. 2.1), we obtain a Cl contribution of 2.6 %.

~~From~~ Based on our simulations, contributions from the tropospheric Cl sink with Cl-Wang (0.6 %) and Cl-Sherwen (1.8 %) are slightly lower than those given in the associated papers (i.e., 0.8 % and 2 %, respectively). This discrepancy is likely due to a slight difference in the definition of the tropopause level or/and in the prescribed OH sink that is used to calculate the total chemical sink.

The tropospheric sink provided by Allan et al. (2007) is well above the other recent values. The tropospheric ~~value from~~ sink estimated by Hossaini et al. (2016), used in recent studies (Saunois et al., 2020; McNorton et al., 2018), is also slightly above that ~~of~~ inferred with Cl-Sherwen (Table 4: 1.4 times higher) but well above ~~that of~~ those inferred with Cl-Wang and Cl-INCA (4 and 8.5 times higher). In the troposphere, the sink ~~induced by~~ inferred with Cl-Taki is much larger than the other sinks (up to 28 times larger) and therefore even larger than the value suggested by Allan et al. (2007) which is already very likely to be overestimated (Gromov et al., 2018). In the stratosphere, ~~the~~ this Cl-Taki sink is also slightly larger than the others (1.3 times that of Cl-Sherwen).

Apart from the Cl-Taki field, ~~we selected here only the fields that provided a realistic range of concentrations when applying~~ all the fields provide a range of tropospheric concentrations that are roughly in line with the conclusions of Gromov et al. (2018). ~~We therefore consider only the Cl fields that give a tropospheric oxidation below 2 % as realistic. These fields happen to be the most recent and up-to-date estimations.~~ In the stratosphere, all tested fields ~~are considered realistic because they~~ provide an oxidation between 1.1 and 1.6 %, ~~therefore~~ in agreement with Saunois et al. (2020) and McCarthy et al. (2003) (0.4-2.4 %). ~~In the following analysis, results from SimTaki are presented only to illustrate why a Cl field should be rigorously analyzed (concentration, oxidation) before prescribing it in a forward or inverse simulation.~~

Table 4. Percentage of contribution from Cl oxidation to total chemical oxidation (Cl, O(^{1}D) and OH)~~and~~, sink ~~intensity~~ intensities and mean Cl concentration (conc.). Values are given for the tropospheric, stratospheric and total (tropospheric + stratospheric) Cl sinks for several fields, either used in the simulations or in other studies. * Values taken from literature. H16 : Hossaini et al. (2016) ; A07 : Allan et al. (2007) ; P11 : Patra et al. (2011)

Field	Troposphere			Stratosphere			Total	
	Oxidation	Sink	Conc.	Oxidation	Sink	Conc.	Oxidation	Sink
	(%)	(TgCH$_4$.yr^{-1})	(molec.cm^{-3})	(%)	(TgCH$_4$.yr^{-1})	(molec.cm^{-3})	(%)	(TgCH$_4$.yr^{-1})
~~SimNoCl~~ INV-NoCl	0	0	0	0	0	0	0	0
~~SimNoTropo~~ INV-NoTropo	0	0	0	1.1	~~6.1~~ 5.8	1.5×10^5	1.1	~~6.1~~ 5.8
~~SimINCA~~ INV-INCA	0.3	~~1.5~~ 1.4	3.3×10^2	1.0	~~5.2~~ 5.0	1.4×10^5	~~1.2~~ 1.3	~~6.7~~ 6.4
~~SimREF~~ INV-Wang	0.6	~~3.2~~ 3.0	6.1×10^2	1.1	~~6.1~~ 5.8	1.5×10^5	1.7	~~9.3~~ 8.8
~~SimSherwen~~ INV-Sherwen	1.8	~~9.9~~ 9.3	1.1×10^3	1.2	~~6.4~~ 6.0	1.6×10^5	3.0	~~16.3~~ 15.3
H16*	2.6	12-13	1.3×10^3	N/A	N/A	N/A	N/A	N/A
A07*	5	25	N/A	N/A	N/A	N/A	N/A	N/A
~~SimTaki~~ INV-Taki	8.5	~~47.0~~ 46.8	4.7×10^3	1.6	~~9.0~~ 8.9	2.1×10^5	10.1	~~56.0~~ 55.7
P11*	N/A	N/A	N/A	1.3-2.6	6.8-13.7	N/A	N/A	N/A

3.2 ~~CH$_4$ surface concentrations~~ Spatial distributions of biases

~~The impact of the Cl sink on~~ Figure 2 shows the CH$_4$ ~~mole fractions is analyzed by comparing the simulations against SimREF at MBL station locations providing~~ and δ^{13}C(CH$_4$) ~~data. Since the Cl fields vary mainly as a function of latitude,~~ surface absolute biases between the simulations and the FWD-Wang averaged over the period 2010-2018. For CH$_4$, globally-averaged

13

biases range from -18 ppb to 123 ppb because prescribed Cl sinks are distinct. However, the spatial variations of biases around their mean value are similar for FWD-Taki, FWD-INCA and FWD-Sherwen since all the fields exhibit similar spatial patterns. For all biases, the minimum-maximum relative difference is below 5 %. Some biases are low enough for us to see the influence of surface fluxes (local CH_4 enhancements) on biases in Fig. 2 (blue tropical regions in FWD-INCA and FWD-NoTropo panels). This is not visible in the bias corresponding to FWD-Sherwen and FWD-Taki as the ~~comparisons are made by averaging values over bands of latitude.~~Here, the bias b is defined as :

$$b_{X,i,l} = \overline{X_{i,s} - X_{\text{SimREF},s}}^{\,l}$$

minimum-maximum difference is larger. Tropospheric Cl concentrations are generally larger in the tropics and therefore the bias between FWD-NoTropo and FWD-Wang is also larger in this latitudinal band. However, further removing the stratospheric Cl (FWD-NoCl) invert the spatial distribution of the bias, hence leading to higher values in the polar regions. Following the Brewer-Dobson circulation, stratospheric air descends into the troposphere mainly in polar regions (Butchart, 2014). The influence of stratospheric Cl on tropospheric CH_4 mole fractions is therefore enhanced in these regions. To summarize, although spatial variations exist and can be slightly different from one field to another, they generally remain below 1 ppb and can be neglected.

~~where $b_{X,i,l}$ is the bias for a specific quantity X (i. e. , or~~ As for $\delta^{13}C(CH_4)$~~), a specific simulation i, and a specific band of latitude l. $X_{i,s}$ denotes the or~~, globally-averaged biases are larger than the recent global decline in $\delta^{13}C(CH_4)$ ~~values simulated by a simulation i and at a station s. The $\overline{(.)}^{\,l}$ symbol indicates the mean over all the stations whose location is inside the band of latitude l.~~

~~In a box model, the temporal evolution of the~~ observed since 2007 (Nisbet et al., 2019). Although mean values highly differ from one simulation to another, spatial variations are very similar and we find the lowest values where the sources with the most depleted isotopic source signatures are located, e.g., in boreal regions (wetlands) and in Asia (agriculture and waste). These spatial discrepancies are mainly caused by the non-linear effects associated with isotopes. In a very simple framework, we can demonstrate that the steady-state bias $\Delta\delta_a$ between two simulations prescribing the same CH_4 ~~budget for a simulation i is described by the equation below :~~source and the same source signature δ_s is given by the formula :

$$\frac{dB_i}{dt} = S\Delta\delta_a \approx -\frac{B_i}{\tau_i}\Delta\varepsilon \cdot (1 + \delta_s) \tag{2}$$

~~where B_i is the mass of in the atmosphere in , S is the source in and τ_i is the chemical lifetime of in the atmosphere in . Note that the same sources are prescribed for all simulations. The temporal evolution of the budget is not linear, because the sink is proportional to mole fractions. decrease/increase induces a negative feedback on the magnitude of the sink, leading to a stabilization of~~ $\Delta\varepsilon$ denotes the difference of prescribed fractionation between the two simulations due to differences in Cl concentrations. More information and a comprehensive demonstration are provided in Text S4. Consequently, the bias will be lower if the source is more depleted in ^{13}C. Figure 2 confirms that these non-linear effects have a larger influence on the spatial patterns of the bias than stratospheric air intrusions, spatial differences between Cl concentrations or even horizontal transport. In addition, the ~~mass of after several decades if S~~ bias between FWD-NoTropo and ~~τ_i are constant over time. Here, the bias~~

14

~~between two simulations is caused by a change in τ because we modify the Cl field. The evolution of the bias b can therefore be described by the equation :~~

$$\frac{db}{dt} = \frac{d(B_2 - B_1)}{dt} = -\frac{B_1}{\tau_1} + \frac{B_2}{\tau_2}$$

~~However, in~~ FWD-NoCl is a ~~surface-based inversion (i.e., an inversion assimilating observations from surface stations) without sink optimization, the bias is compensated by a correction of the global surface flux $S + \Delta S$. The inversion system therefore answers the question : "What is the~~ good proxy for quantifying the influence of stratospheric Cl on δ^{13}C(CH$_4$) at the surface. At the end of the period, STE cause a globally-averaged increase of δ^{13}C(CH$_4$) at the surface of 0.30 ± 0.01 ‰ (depending on the region) when the stratospheric Cl concentrations from Wang et al. (2021) are adopted. Although this value could change with another field, our range of stratospheric Cl concentrations is small and the Cl-Wang field is taken from the most comprehensive and recent study to date. Therefore, we think that this value is a good estimate of the contemporary influence of stratospheric Cl on δ^{13}C(CH$_4$) at the surface. It is larger than the estimate of Wang et al. (2002) inferred between 1970 and 1992 (0.23 ‰). Both our estimates were obtained after running a model for about the same amount of years, therefore these values are comparable. In addition, Wang et al. (2002) experimented with multiple configurations. In particular, one of the runs tested an enhanced STE, resulting in a value of ~~ΔS that will offset the bias caused by~~ 0.38 ‰. Another test, with stratospheric Cl concentrations increased by a factor 2, provided a value of 0.32 ‰. However, the latter study does not provide an estimate of the mean stratospheric Cl concentration. It is therefore difficult to know whether the discrepancy between both estimates are due to Cl stratospheric concentrations, the rate of STE or something else. Our value however lies within the full range obtained by Wang et al. (2002).

3.3 Global CH$_4$ flux adjustment

The global CH$_4$ flux adjustments resulting from a change in ~~the prescribed sink ?". The temporal evolution of the bias between a simulation~~ Cl sink have been derived using the three methods introduced in Sect. 2.5 (Fig. 3). The INV-Wang simulation has been chosen as a reference. Global CH$_4$ flux adjustments range from -7.0 TgCH$_4$.yr^{-1} (no Cl sink) to $+46.8$ TgCH$_4$.yr^{-1} (Cl-Taki) with M1. Small differences between M1 and the other methods exist (up to 10%). However, the strong similarity between these results confirms that M2 and M3 can be employed to investigate the influence of the Cl sink on inversion-based adjustments for the global scale without significantly impacting the magnitude or sign of the results. This result corresponding to Cl influence may not be valid for larger changes such as those resulting from an OH sink modification. With the M1 method, more information about the spatial characteristics of the flux adjustment can be provided. About 70 % of the adjustment is made in the ~~reference simulation can therefore be described by the equation :~~

$$\frac{db}{dt} = \Delta S - \frac{b}{\tau_{ref}}$$

~~τ_{ref} denotes the chemical lifetime in the reference simulation. We consider that ΔS is constant over time as the inter-annual variability of the Cl sink is below 0.4 . In that case,~~ tropics (30°S-30°N) and the rest in the northern mid-latitudes (30°N-60°N).

The other regions of the ~~solution of this equation is :~~

$$b(t) = \Delta S \times \tau_{ref} \times (1 - e^{-\frac{t}{\tau_{ref}}})$$

~~The value of ΔS can be obtained by analyzing the temporal evolution of the bias and, in particular, by looking at the value of the bias when it is stabilized (steady state). Here, after 21 years of simulation, the stabilization is not reached yet (see Fig. ??, top row). Therefore, we choose to extend our results by applying a curve fitting function to our simulated values :~~

$$b_{X,i,l}(t) = A_{X,i,l} \times B_{X,i,l} \times (1 - e^{-\frac{t}{B_{X,i,l}}})$$

~~$A_{X,i,l}$ and $B_{X,i,l}$ are two constants that the curve fitting algorithm returns~~ world contribute only to a few percents of the global adjustment. This is consistent with the spatial distribution of the biases presented in Sect. 3.2. Also, changing the reference scenario does not modify this distribution.

Using this sample of results, we have also build a linear regression model in order to ~~maximize the agreement between the simulated values and the curve fitting function. Using this function, the results are extended until 2070 to reach a clear stabilization of simulated biases (see Fig. ??, top row).~~

~~At steady state, the bias of~~ easily predict the influence of changing the Cl field on the global CH_4 ~~at the surface varies between -20.0~~flux adjustment. By performing a linear regression between the adjustment values inferred with M1 and the mean tropospheric Cl concentrations, we obtain a coefficient of determination R^2 very close to 1. It indicates that a linear relationship is a very good approximation of the relationship between the two variables. Consequently, one can affirm that each increase by 1000 ~~for SimSherwen and 24.5 for SimNoCl (Table ??, second column). An estimation of ΔS is given by the coefficient $A_{X,i,l}$. It provides a result in . To convert this value in , we use a conversion factor of 2.767 (Lassey et al., 2000) and show the final estimates in Table ??, fourth column. For SimNoCl and SimSherwen, these estimations are~~ molec.cm^{-3} in the mean tropospheric Cl concentration would require an adjustment of $+11.7$ TgCH$_4$.yr^{-1}. It represents a change in about 2 % of total CH_4 atmospheric oxidation, which is very small compared to the current uncertainties in OH sink intensity and their influences on top-down estimates (Zhao et al., 2020, 2019). Furthermore, the discrepancies between the mean tropospheric Cl concentrations estimated by recent studies are generally smaller than 1000 molec.cm^{-3}. Therefore, the uncertainty on CH_4 emission estimates arising from the choice of Cl sink should not be larger than 11.7 TgCH$_4$.yr^{-1}. However, inverse modellers should be extremely cautious before using Cl fields that exhibit much larger Cl concentrations than recent estimates. As shown here, it can cause the flux adjustment to reach 50 TgCH$_4$.yr^{-1}.

As the inversion compensates for the sink difference induced by a change from one field (Cl-1) to another (Cl-2), the numerical value of the global flux adjustment is very close (~~difference of less than 0.2~~ less than a 10 % difference) to the ~~tropospheric Cl sink discrepancies from Table 4. Indeed, as the stratospheric Cl sinks in SimREF, SimINCA, SimNoTropo and SimSherwen are almost identical, the biases induced by tropospheric Cl sink discrepancies will be logically compensated by a source adjustment of the same intensity as the sink discrepancy. For SimNoCl, the biases at the surface are also influenced by large stratospheric sink discrepancies. Therefore, the inferred adjustment values cannot be so simply related to the sink discrepancies. Also, latitude has a very low influence on biases and adjustment values, causing a variation of less than 5 % around the mean value (see Fig. ??).~~

We conclude that a source adjustment of 12.3 difference between estimated tropospheric sink intensities for Cl-1 and Cl-2 (see Table 4). The stratospheric sink appears to have also a small influence on the results. For instance, between INV-NoCl and INV-NoTropo, there is a global flux adjustment of 3.8 $TgCH_4.yr^{-1}$ would be necessary between a surface-based inversion without Cl sink, such as the inversions carried out with LMDz-SACS up to now, and a surface-based inversion adopting the Cl-Sherwen field. Saunois et al. (2020) obtained an uncertainty on the total, resulting only from the difference in stratospheric Cl sink. It is significantly smaller than the stratospheric sink itself because a fraction of CH_4 fluxes of about 40 does not return to the troposphere from the stratosphere. In addition, stratospheric influence is not always the only cause of discrepancies. For instance, the global flux adjustment obtained with INV-Taki is 48.8 ± 5.8 $TgCH_4.yr^{-1}$ (maximum - minimum difference) across the different top-down inversions reported. The difference in the Cl configuration between the multiple inversions of Saunois et al. (2020) may have contributed to the uncertainty they estimated. Although the adjustment value we obtain here thus remains lower than the uncertainty generated by the different configurations used in Saunois et al. (2020), it is not negligible as we make the point that this source adjustment could be much larger if an unrealistic Cl field was used. For example, prescribing the and the difference between the estimated total (tropospheric and stratospheric) sinks is 47.0 ± 0.8 $TgCH_4.yr^{-1}$. Therefore, differences between the estimated sinks cannot explain alone the global flux adjustment. It is very likely that if the spatial distributions of two tropospheric Cl sinks are different, it can cause such discrepancies. Cl-Taki field instead of the Cl-Wang field would result in an adjustment value of 48.1 . If a single Cl configuration for all inversions could be agreed upon, this would likely lead to a reduction of the uncertainty on emission fluxes infers a larger proportion of its total sink in the tropics compared to Cl-Wang. However, the total chemical lifetime of CH_4 is smaller in the tropics than in the high-latitudes. Therefore, the inversion system must increase even more the CH_4 flux in this region to compensate for these spatial distribution discrepancies. This effect remains nevertheless extremely small. For the other simulations, it is very difficult to separate the influence of the stratospheric sink from the influence of discrepancies arising from spatial distribution.

As the stratospheric Cl concentrations estimated by the models presented here suffer much less uncertainties than the tropospheric Cl concentrations, we did not investigate the influence of the variations in stratospheric Cl. However, note that M2 and M3 have difficulties reproducing the M1 value when we remove entirely the Cl sink (NoCl bars in Fig. 3). It confirms that the stratospheric influence of Cl cannot be well captured by a box model framework.

Global adjustment values of source and isotopic signatures inferred from and biases at the surface. Second column is the global bias at the surface and at steady state. Third column is the global bias at the surface and at steady state. Fourth column is the global source adjustment value estimated using the methods described in Sect. **??**. Fifth column is the $_{source}$ adjustment value estimated using the methods described in Sect. **??**. Latitudinal dependency is reported as a minimum-maximum range min/max for all values. Flux Signature () () () () SimNoCl 24.5 24.4 / 24.8 −0.66 −0.70 / −0.63 −5.7 −5.7 / −5.70.66 0.63 / 0.70SimNoTropo 10.0 10.0 / 10.0 −0.30 −0.31 / −0.28 −3.2 −3.2 / −3.20.30 0.28 / 0.31SimINCA 8.6 8.6 / 8.8 −0.25 −0.26 / −0.24 −1.9 −2.0 / −1.90.25 0.24 / 0.26SimSherwen −20.0 −21.2 / −20.50.60 0.59 / 0.626.6 6.5 / 6.8 −0.60 −0.62 / −0.59SimTaki −140.1 −142.2 / −138.24.13 4.01 / 4.2448.1 46.9 / 49.2 −4.13 −4.24 / −4.01

3.4 Global $\delta^{13}C(CH_4)$ signal at the surface $_{source}$ source signature adjustment

17

In contrast with the biases, the biases between the simulations are much larger than recent observed downward shifts (∼ 0.3Our methods are also designed to derive the global δ^{13}C(CH$_4$)$_{source}$ source signature adjustment resulting from a change in prescribed Cl field. Figure 3 provides a comparison of the results with the three different methods. Global δ^{13}C(CH$_4$)$_{source}$ adjustments range from -4.1‰ since 2007) . We use the same curve fitting method as before to propagate the time-series until 2070 in order to reach a steady state (see Fig. **??**, bottom row) .

SimNoTropo, SimINCA, SimREF and SimSherwen have very similar stratospheric Cl sinks (Table 4). Therefore, biases for SimNoCl, SimNoTropo, and SimSherwen are mostly generated by discrepancies in tropospheric Cl sink intensity. We can estimate that each percent increase in how much is oxidized by Cl leads to an additional 0.53 (Cl-Taki) to $+0.6$‰ increase in , therefore larger than the global downward shift observed since 2007. After 14 years of simulation, we obtain a value of 0.46 , (no Cl sink) with M1. M2 and M3 results are highly consistent with M1 results, showing that simpler methods can also capture the δ^{13}C(CH$_4$)$_{source}$ adjustment. A linear regression model has also been built to quantify the relationship between the δ^{13}C(CH$_4$)$_{source}$ adjustment and the mean tropospheric Cl concentration. We obtain a coefficient of determination R^2 very close to the value of 0.51 and estimate that a δ^{13}C(CH$_4$)$_{source}$ adjustment of -1.0‰ inferred by Strode et al. (2020) after the same number of years.

Stratospheric Cl also influences at the surface through STE. We estimate this influence using the bias between SimNoCl and SimNoTropo. Intrusions of stratospheric air are therefore responsible of an enrichment at the surface stations of 0.30 ± 0.01would result from each increase by 1000 (depending on the latitude)after 21 years of simulation, larger than the value of Wang et al. (2002) inferred between 1970 and 1992 (0.23molec.cm^{-3} in the mean tropospheric Cl concentration to compensate for the enhanced atmospheric isotopic fractionation. Based on the Cl fields analyzed here, the globally-averaged δ^{13}C(CH$_4$)$_{source}$ should very likely lie in the range of $[-56.7, -51.9]$‰) .

To reduce these biases to zero, an inversion system would adjust the globally-averaged isotopic signature of the sources, denoted by $_{source}$. This adjustment factor would be roughly equal to the opposite of the bias at steady state (see demonstration in the supplementary Text S2). It would therefore oscillate between . If one excludes outliers such as Cl-Taki or no Cl at all, we deduce a likely range of $[-0.60$53.1, $-52.2]$‰ (SimSherwen)and $+0.66$for the period 1998-2018. This range does not account for other uncertainties, e.g., uncertainties in the numerical value of the KIE associated with the OH sink.

We find a difference of 0.30‰ (SimNoCl) around the mean isotopic signature of the between global δ^{13}C(CH$_4$)$_{source}$ inferred with INV-NoCl and INV-NoTropo, confirming the influence of stratospheric Cl on δ^{13}C(CH$_4$) at the surface first estimated in Sect. 3.2. This effect must be rigorously accounted for when using one-box modelling to estimate global CH$_4$ source prescribed in SimREF. We would therefore obtain, after the inversion process, a mean global signature between -53.20 (SimSherwen)and -51.94 (SimNoCl).

The system would modify emissions and dealing with isotopic constraints because it is comparable to the recent global decline in δ^{13}C(CH$_4$) observed since 2007 (Nisbet et al., 2019). These results highlight that preferring a Cl field over another can highly influence the posterior globally-averaged δ^{13}C(CH$_4$)$_{source}$ by changing of an inversion performed with isotopic constraints. As the globally-averaged δ^{13}C(CH$_4$)$_{source}$ mainly depends on the source mixtureand/or the isotopic signatures of the multiple emission categories , with a weight depending on uncertainties associated to both. For instance, an adjustment

18

~~of −0.60 could be made by increasing the wetlands share from 32 %,~~ contributions from emission categories ~~to 43 % or by shifting the mean isotopic signature of wetlandsfrom −56.6 to −58.5 , more in agreement with recent estimates (Ganesan et al., 2018; Sherwood et al., 2017) than our inverted value (see Table ??). However, the system would likely change not only wetlands but all emission categories, possibly limiting an unlikely large change in wetlands emissions only. Nevertheless, the configuration used to represent the Cl sink could largely influence the result of an inversion assimilating both and~~ total emissions can be highly affected by a modification of the prescribed Cl field. In our inversions, WET, BB, FFG and AGW emissions contribute between [32.5, 33.3] %, [4.9, 5.2] % [21.0, 21.5] % and [37.3, 37.6] %, respectively. For wetlands, such a variation roughly corresponds to a 15 $TgCH_4.yr^{-1}$ change, resulting only from uncertainties in Cl concentrations. Furthermore, our inversions optimize the source signatures prescribed for each category and account for a relatively large uncertainty in prior estimates. Consequently, it releases part of the constraint that could be applied on the source mixture in an inversion not optimizing source signatures. Our results are therefore a lower-bound estimate of the influence of the Cl sink on top-down estimates with isotopic constraints. It emphasizes how careful one must be when selecting a prescribed Cl field for running such inversions.

~~Seasonal cycles of and biases between the surface values simulated by the various simulations (see Sect. ??) and those simulated by SimREF. The biases are averaged over four bands of latitude.~~

3.5 CH_4 and $\delta^{13}C(CH_4)$ seasonal cycles

~~To investigate the seasonal cycle, the simulations are compared against SimREF by averaging values over latitudinal bands~~ The peak-to-peak amplitude of the CH_4 seasonal cycle simulated by FWD-Wang at the surface typically ranges between 5 and 120 ppb, depending on the region (see Fig. ~~??) as in Sect. ?? and ??.~~

~~With the realistic Cl fields tested here, the influence on the seasonal cycle is negligible regardless of the latitudinal band analyzed. The variation in the seasonal cycle amplitude due to Cl is about 0.4 ppb whereas the seasonal cycle amplitude is about 20 in the Southern Hemisphere and 30~~ S6, in the supplement). It is larger where wetlands and biomass burning emissions are located because both sources exhibit a very strong seasonal dependence. Apart from using the Cl-Taki, changing the prescribed Cl field does not modify the amplitude and the spatial variability of the CH_4 seasonal cycle. Compared to FWD-Wang, the variation is below 3 % in both hemispheres for FWD-Sherwen, FWD-INCA, FWD-NoTropo and FWD-NoCl. However, it can reach 10 % in the Northern Hemisphere ~~. The variation therefore accounts for 1-2 % of~~ when applying Cl-Taki instead of Cl-Wang.

As for $\delta^{13}C(CH_4)$, the seasonal cycle amplitude ~~.~~

~~The impact is more important for the~~ simulated by FWD-Wang typically ranges between 0.05 and 0.65 ‰. Again, changing the prescribed Cl field has more influence on $\delta^{13}C(CH_4)$ ~~seasonal cycle and is dependent on latitude. In~~ than on CH_4. For instance, in the Southern Hemisphere, the variation in amplitude ~~between SimREF and SimSherwen~~ when switching from Cl-Wang to Cl-Sherwen is about 0.02 ‰, which represents 20 % of the total seasonal cycle amplitude. In the Northern Hemisphere, the variation can exceed 0.03 ‰, ~~which represents~~ but it represents only 10 % of the seasonal cycle amplitude.

555 ~~SimTaki (not shown on Fig. ?? for clarity reason) causes a much larger variation in seasonal cycle for both and . For ,~~ ~~variations reach 5~~Adopting the Cl-Taki field drastically increases this variation in the amplitude of the seasonal cycle: variations can go up to 99 % in the Southern Hemisphere and ~~10~~58 % in the Northern Hemisphere~~. As~~, with large spatial disparities. Also, differences of amplitudes for δ^{13}C(CH$_4$) ~~, variations go up to 99~~between INV-NoTropo and INV-NoCl reach 10 % in the ~~Southern Hemisphere and 58 % in the Northern Hemisphere~~tropics and are negligible in other regions. It indicates that STE

560 tends to slightly increase the seasonal cycle around the equator when stratospheric Cl is included.

The influence of Cl on the simulated δ^{13}C(CH$_4$) seasonal cycle must be considered as it ~~will impact~~ impacts the results of an inversion with ~~data assimilation~~isotopic constraints. A misrepresentation of the seasonal cycle forces the system to adjust the intensity of sources that ~~actively participate in~~ exert a large influence on the seasonal cycle, such as wetlands or biomass burning~~emissions. This influence is negligible for and noticeable for when keeping realistic Cl concentrations but becomes~~

565 ~~very large when using other Cl fields, such as the Cl-Taki field.~~ Using the M1 method presented above, one can analyze the influence of prescribed Cl sink on optimized emissions for all categories. Apart from INV-Taki, the variation of peak-to-peak amplitude of the seasonal cycle for global emissions and for each category is small between INV-Wang and all the other inverse configurations. It is below 5 % for WET, AGW, NAT and FFG but can reach 10 % for BB. On the contrary, INV-Taki infers much larger amplitude changes. BB, WET, AGW, NAT and FFG seasonal cycle amplitudes are increased by 3.1, 2.0, 0.1, 0.1

570 and 0.2 TgCH$_4$.yr^{-1} (134, 14, 9, 1 and 21 %), respectively.

3.6 CH$_4$ vertical profiles

~~Vertical~~ At present, vertical profile measurements of CH$_4$ are too scarce to be considered as a stand-alone constraint in inversion systems, and so are rather used as evaluation data. Nevertheless, as their accuracy, spatial coverage and number increase, their assimilation will become increasingly relevant. It is, however, necessary to increase the model-observation agreement,

575 especially in the stratosphere, before considering their assimilation. We analyze here the influence of the Cl ~~configuration~~ ~~on these~~ distribution on the simulated profiles. We also compare the simulated vertical profiles to observations to investigate whether modifying the Cl ~~configuration~~ distribution can help to reduce the model-observation discrepancies.

Simulated vertical profiles are sampled at the same locations and ~~time as the observations available . The bias b_{X,y,p,d_1,d_2}~~ ~~between two vertical profiles d_1 and d_2 (simulated or observed)~~times as the available observations. Simulations with optimized

580 fluxes (INV-*) are used to reduce the influence of a potential tropospheric bias resulting from a poor estimation of the CH$_4$ fluxes and to analyze to what extent a station-based inversion can help to reduce both the tropospheric and stratospheric biases.

The bias b_p between observed (obs) and simulated (sim) values for a specific profile p ~~, a specific quantity X (i.e., and for~~ $X = $ CH$_4$ ~~) and~~ is given by:

585 $$b_p = X_{p,sim} - X_{p,obs} \tag{3}$$

20

We define the mean bias $\overline{b_{k,P}}^{y}$ for a specific layer ~~y~~ (troposphere, stratosphere or total ~~) is given by:~~

$$b_{X,y,p,d_1,d_2} = \overline{X_{d_1,p} - X_{d_2,p}}^{y}$$

~~The $\overline{(.)}^{y}$ symbol indicates the mean~~ column) and a specific region of interest r as the root-mean square difference (RMSD) over all the ~~vertical levels in the layer y. We also define the mean bias as the bias averaged over all available vertical profiles :~~

$$\overline{b_{X,y,d_1,d_2}} = \overline{b_{X,y,p,d_1,d_2}}^{p}$$

values of the bias in this layer and in this region.

Table 5. ~~Mean bias relative to SimREF for~~ RMSD between simulated and observed CH$_4$ vertical profiles in the troposphere and stratosphere ~~as well as in~~ for different regions of the ~~Northern and Southern Hemisphere~~ world.

	Troposphere				Stratosphere			
	Northern high-latitudes	Mid-latitudes USA	Mid-latitudes Europe	Southern Hemisphere	Northern high-latitudes	Mid-latitudes USA	Mid-latitudes Europe	Southern Hemisphere
Simulation	ppb							
~~SimNoCl~~ INV-Wang	3.0	15.6	21.9	16.7	106.8	81.4	93.0	67.4
INV-Taki	2.3	16.0	19.3	~~19.1~~ 15.1	~~50.8~~ 111.7	~~38.9~~ 75.4	86.2	71.6
~~SimNoTropo~~ INV-Sherwen	~~10.9~~ 2.9	~~10.8~~ 14.6	~~15.2~~ 22.4	~~12.9~~ 15.4	109.8	81.6	93.2	69.0
~~SimINCA~~ INV-INCA	~~6.8~~ 3.3	~~6.7~~ 16.2	~~11.8~~ 21.7	~~9.2~~ 17.6	108.6	86.2	98.2	66.9
~~SimSherwen~~ INV-NoTropo	~~−18.7~~ 3.5	~~−18.2~~ 16.3	~~−18.1~~ 21.7	~~−17.9~~ 17.4	106.6	81.1	92.5	67.2
~~SimTaki~~ INV-NoCl	~~−129.7~~ 4.4	~~−125.0~~ 17.0	~~−118.5~~ 21.8	~~−121.4~~ 18.4	115.5	103.6	118.6	67.5

~~The mean bias relative to SimREF is given for all simulations and observations in Table **??**. A change in the Cl field (and keeping it realistic) induces a maximum mean bias of 51 in the stratosphere (SimNoCl). For all simulations besides SimNoCl, the bias is roughly constant over the entire column (see Fig. **??**), because the Cl concentrations in the stratosphere are very similar. Also, a change in the tropospheric Cl sink influences tropospheric and stratospheric values to the same magnitude. For SimNoCl, the bias is constant in the troposphere but starts increasing above 15 km at 7.5 in the Northern Hemisphere and 7 in the Southern Hemisphere. At 25 km, the bias therefore reaches 130 ppb in the Northern Hemisphere for this simulation~~

Table 5 shows the mean bias for four regions of the world where vertical profiles have been observed : northern high-latitudes in Europe, mid-latitudes in Europe, mid-latitudes in the USA and Southern Hemisphere (Oceania). After inversion adjustments, tropospheric CH$_4$ is well captured by the model. Biases are particularly low in the northern high-latitudes, albeit the number of profiles (4) is much lower in this region and additional data should be used to confirm this result. In the other regions, values are larger mainly because models have difficulties reproducing observed values very close to the surface. It is likely due to a problem of representation of transport in the boundary layer in LMDz-SACS and/or a problem of spatial representativity of sources that can be resolved only by increasing spatial resolution. Simulated profiles are generally slightly overestimated in Europe and underestimated in the USA in the troposphere, albeit by less than 10 ppb. Overall, the prescribed Cl field has very

little impact on the tropospheric mean biases. Discrepancies between Cl fields for a given region are too small to validate one Cl field over another.

Mean biases are much larger in the stratosphere, ranging from about 67 ppb in the southern high-latitudes to 115 ppb in the northern high-latitudes. Outside the northern high-latitudes, simulated values are generally larger than observed values for all simulations and all regions, showing that the model tends to overestimate CH_4 mole fractions, even with optimized fluxes. Influences of the Cl sink are larger in the stratosphere for the four regions. INV-NoCl has more difficulties reproducing the simulated mole fractions above the tropopause, mainly in the Northern Hemisphere, with a mean bias 1.0 to 1.4 times larger than the other simulations. INV-Taki shows the lowest biases in the mid-latitudes, indicating that the stratospheric Cl concentrations could be underestimated in most of the tested fields in this region. However, this overestimation of CH_4 mole fractions in the stratosphere could be also caused by an underestimation of the stratospheric OH or $O(^1D)$ concentrations or a weak transport between troposphere and stratosphere, preventing the tropospheric CH_4 to reach higher altitudes. Such a misrepresentation can also result in an overestimation of the column-weighted average mixing ratio (XCH4) simulated by LMDz-SACS (Ostler et al., 2016). An analysis of XCH4 is however beyond the scope of this study. Overall, modifying the Cl field has a very limited impact on simulated CH_4 vertical profiles as long as its stratospheric concentrations remains in the range analyzed here.

3.7 $\delta^{13}C(CH_4)$ vertical profiles

Figure 5 displays the comparison between observed vertical profiles of $\delta^{13}C(CH_4)$ from Röckmann et al. (2011) and those simulated by the INV-* runs. As most of the observed profiles were retrieved before the beginning of our simulations, we selected the year 2005 for the comparison. Although our inversions did optimize initial conditions, constraints from surface stations do not carry enough information to efficiently optimize stratospheric $\delta^{13}C(CH_4)$. Therefore, a stabilization period in response to the prescribed Cl sink is necessary. However, in the stratosphere, this stabilization is somehow very fast (about 2-3 years) and the year selected for comparison has a negligible influence on the analysis. Selecting 1998 or 1999 slightly influences the comparison but does not affect the conclusions.

640 ~~XCH₄ obtained by remote sensing techniques are now massively assimilated in inversions because satellite observations offer a much larger spatial coverage than in situ measurements. Rigorously estimating the influence of Cl concentrations on a satellite-based inversion would require more than an one-box model approximation. We therefore include only a simple analysis using data from the GOSAT satellite in the supplementary Text S3~~Apart from INV-NoCl, our simulations capture well the observed profiles. Vertical profiles of δ^{13}C(CH₄) that are simulated without any Cl sink are the most inconsistent with available

645 observations. RMSDs of INV-NoCl over KIR, ASA, and GAP are respectively 1.5, 2.2, and 2.5 times higher than the mean RMSD over the other simulations and over the same locations. Furthermore, the differences between Cl-INCA, Cl-Sherwen, Cl-Wang have little influence on the vertical profiles of δ^{13}C(CH₄) due to the fact that the stratospheric Cl concentrations are relatively close (1.4-1.6 $\times$ 10^5 molec.cm^{-3}). Vertical profiles are well captured up to 30-35 km for ASA, HYD, and GAP, confirming that the prescribed Cl concentrations in the lower stratosphere are realistic (average RMSDs of 1.0, 0.5, and 1.5 ‰).

650 Cl-Taki stratospheric concentrations are slightly larger than the others and, therefore, simulated δ^{13}C(CH₄) is higher above 30-35 km for all regions.

   Above KIR, in the polar regions, the simulated values are less consistent with observations (mean RMSD of 4.2 ‰). Several explanations can be given. First, Cl concentrations may be underestimated in the lower stratosphere and in the polar regions. Secondly, the transport between the lower and upper stratosphere may not be correctly represented in the LMDz model, leading

655 to a poor mixing between layers above the tropopause with ^{13}C-enriched CH₄ and more depleted layers below the tropopause. However, there is a high variability in the 7 profiles analyzed above KIR (light gray band), and the simulated values are within the uncertainty of these observations. Overall, available observations are limited to approximately 30 km and the influence of the prescribed Cl sink on the simulations is much clearer above this altitude. It is therefore difficult to prefer one Cl field over another without observing at higher altitudes.

660 **4 Conclusions**

In this study, we tested ~~multiple Cl fields suggested by recent studies~~ a large range Cl concentration fields in order to investigate the influence of the Cl ~~configuration~~ distribution on CH₄ and δ^{13}C(CH₄), and to estimate its potential impact on the estimation of CH₄ sources and isotopic signatures with top-down approaches.

   ~~We tested a realistic range of Cl concentrations, i.e., resulting in Cl tropospheric and stratospheric oxidations that are in~~

665 ~~agreement with recently published studies. We also included a Cl field suggested by the GCP 2018 protocol to be prescribed in inverse simulations in order to investigate its influence on and values in comparison with more realistic and recent Cl fields. The realistic~~ The Cl fields tested here are responsible for between 0.3 % and ~~1.8~~8.5 % of the total CH₄ sink in the troposphere and between 1.0 % and ~~1.2~~1.6 % in the stratosphere.

   ~~At the surface, the change in the Cl field and thus in the associated sink results in a bias in~~ The differences in prescribed Cl

670 concentrations lead to biases in simulated CH₄ mole fractions ~~that reaches a maximum value of 44.5 at steady state. An~~ and δ^{13}C(CH₄) isotopic composition that increase over time but stabilize after several decades.

We develop three methods to predict how an inversion system would adjust ~~the surface fluxes by a value of 12.3~~ global emissions and source signatures in order to compensate for these ~~biases. This adjustment~~ CH$_4$ and δ^{13}C(CH$_4$) biases. The most robust method (M1) provides flux adjustments ranging from -7.0 (no Cl sink) to $+46.8$ TgCH$_4$.yr^{-1} (Cl-Taki). The two

675   other methods yield similar ranges. We show that these adjustment values linearly depend on tropospheric Cl concentrations and that each increase by 1000 molec.cm^{-3} in the mean tropospheric Cl concentration would require an adjustment of $+11.7$ TgCH$_4$.yr^{-1}. However, most of the fields tested here lead to an adjustment below 10 TgCH$_4$.yr^{-1}. It therefore remains small in comparison to the uncertainties inferred by Saunois et al. (2020). ~~However, the use of perhaps more unrealistic Cl fields (as suggested by recent literature) can generate much larger biases.~~

680   ~~values at the surface are also shifted by a change in the prescribed Cl field. In particular, we find an increase in the global mean at the surface of 0.53~~ The same method is applied to quantify the ~~globally-averaged~~ globally-averaged δ^{13}C(CH$_4$)$_{source}$ adjustment. We also find a good linear relationship between the adjustment and the mean tropospheric Cl concentration. A source signature adjustment of -1.0 ‰ ~~at the surface for each additional percent of contribution from the tropospheric Cl sink to the total sink. In an inversion, this additional percent of contribution would reduce the inferred~~ would therefore result from an

685   increase of 1000 molec.cm^{-3} in the mean tropospheric Cl concentration to compensate for the enhanced atmospheric isotopic fractionation. After discarding the Cl-Taki field and the possibility of neglecting the Cl sink, we estimate that the globally-averaged ~~isotopic signature by 0.53~~ source signature ranges from -53.1 to -52.2 ‰. This range represents the uncertainty in globally-averaged source signature resulting from uncertainties in tropospheric Cl concentrations. However, it does not account for other uncertainties, e.g., those related to the KIE of the OH sink. Also, we find that intrusions of stratospheric air

690   are responsible for an enrichment of δ^{13}C(CH$_4$) by 0.30 ‰ at the surface ~~between 1998 and 2018. Neglecting the influence of stratospheric Cl on~~ in comparison with an atmosphere without stratospheric Cl. We also show here that the choice of the Cl field has a very strong influence on the source mixture obtained with an inversion assimilating δ^{13}C(CH$_4$) ~~surface values could therefore increase the global mean isotopic signature estimated by an inversion by 0.30~~ observations.

   ~~seasonal cycles are only slightly influenced by a~~ A modification of the Cl ~~sink (1-2 % change in the seasonal cycle amplitude).~~

695   ~~Changing the Cl field~~ field within the tested range only slightly influences CH$_4$ seasonal cycles. It can nevertheless modify the amplitudes of δ^{13}C(CH$_4$) seasonal cycle by up to 10-20 % for most of the tested fields, depending on the latitude. To compensate for this change in seasonal cycles, an inversion system might reduce or amplify the seasonal cycles of each emission categories, in particular those which have a large impact on the δ^{13}C(CH$_4$) seasonal cycle, namely wetlands and biomass burning.

700   We also investigate the influence of Cl concentrations on the modeling of CH$_4$ and δ^{13}C(CH$_4$) vertical profiles. ~~We find that statospheric model-observation~~ Observed profiles are well captured by the model, although simulated CH$_4$ mole fractions are generally larger than observed values above the tropopause. We conclude that these discrepancies in LMDz-SACS are unlikely to be caused by a misrepresentation of the Cl sink~~, although a change in Cl concentrations can shift mole fractions at 25 km by up to 130 . Also, a change in the tropospheric Cl sink influences tropospheric and stratospheric mole fractions to the same~~

705   ~~magnitude.~~

   ∴

It is difficult to conclude which Cl field provides the most realistic representation of the Cl sink among those tested here. Recent developments and efforts have nevertheless narrowed the range of uncertainties regarding the Cl concentrations (less than 1.1×10^3 molec.cm^{-3} in the troposphere and 1.4-1.6 $\times 10^5$ molec.cm^{-3} in the stratosphere). Our study shows that the impact of a change in Cl field on top-down CH_4 flux estimates should be small compared to current uncertainties in Saunois et al. (2020) if this change is made within ~~a realistic~~ the range of Cl concentrations ~~both in the troposphere and the stratosphere~~recently estimated. A Cl ~~configuration~~ distribution for all inversions agreed upon in multi-model studies such as Saunois et al. (2020) should ~~however~~ reduce the spread in estimated CH_4 ~~emission~~ fluxes. We ~~show that the choice of the Cl field is however critical (both in the troposphere and the stratosphere) for the global estimates of an inversion assimilating observations and can lead to radically different source mixtures and/or source signatures~~suggest to adopt recent estimates, especially that of Wang et al. (2021) which results from the most comprehensive study to date.

References

Allan, W., Struthers, H., and Lowe, D. C.: Methane carbon isotope effects caused by atomic chlorine in the marine boundary layer: Global model results compared with Southern Hemisphere measurements, Journal of Geophysical Research, 112, https://doi.org/10.1029/2006JD007369, 2007.

Baier, B., Sweeney, C., T., N., Higgs, J., Wolter, S., and Laboratory, N. G. M.: NOAA AirCore atmospheric sampling system profiles (Version 20181101) [Data set], NOAA GML, https://doi.org/10.15138/6AV0-MY81, 2021.

Bousquet, P., Ciais, P., Miller, J. B., Dlugokencky, E. J., Hauglustaine, D. A., Prigent, C., Van der Werf, G. R., Peylin, P., Brunke, E.-G., Carouge, C., Langenfelds, R. L., Lathière, J., Papa, F., Ramonet, M., Schmidt, M., Steele, L. P., Tyler, S. C., and White, J.: Contribution of anthropogenic and natural sources to atmospheric methane variability, Nature, 443, 439–443, https://doi.org/10.1038/nature05132, 2006.

Burkholder, J. B., Abbatt, J. P. D., Huie, R. E., Kurylo, M. J., Wilmouth, D. M., Sander, S. P., Barker, J. R., Kolb, C. E., Orkin, V. L., and Wine, P. H.: JPL Publication 15-10: Chemical Kinetics and Photochemical Data for Use in Atmospheric Studies, p. 1392, 2015.

Butchart, N.: The Brewer-Dobson circulation, Reviews of Geophysics, 52, 157–184, https://doi.org/10.1002/2013RG000448, _eprint: https://onlinelibrary.wiley.com/doi/pdf/10.1002/2013RG000448, 2014.

Cantrell, C. A., Shetter, R. E., McDaniel, A. H., Calvert, J. G., Davidson, J. A., Lowe, D. C., Tyler, S. C., Cicerone, R. J., and Greenberg, J. P.: Carbon kinetic isotope effect in the oxidation of methane by the hydroxyl radical, Journal of Geophysical Research: Atmospheres, 95, 22 455–22 462, https://doi.org/doi.org/10.1029/JD095iD13p22455, 1990.

Chevallier, F., Fisher, M., Peylin, P., Serrar, S., Bousquet, P., Bréon, F.-M., Chédin, A., and Ciais, P.: Inferring CO_2 sources and sinks from satellite observations: Method and application to TOVS data, Journal of Geophysical Research, 110, https://doi.org/10.1029/2005JD006390, 2005.

Craig, H.: Isotopic standards for carbon and oxygen and correction factors for mass-spectrometric analysis of carbon dioxide, Geochimica et Cosmochimica Acta, 12, 133–149, https://doi.org/10.1016/0016-7037(57)90024-8, 1957.

Dlugokencky, E. J.: NOAA/GML, www.esrl.noaa.gov/gmd/ccgg/trends_ch4/, last access : 12 July 2021, 2021.

Dlugokencky, E. J.: NOAA/GML, www.esrl.noaa.gov/gmd/ccgg/trends_ch4/, last access : 9 May 2022, 2022.

Etheridge, D. M., Steele, L. P., Francey, R. J., and Langenfelds, R. L.: Atmospheric methane between 1000 A.D. and present: Evidence of anthropogenic emissions and climatic variability, Journal of Geophysical Research: Atmospheres, 103, 15 979–15 993, https://doi.org/10.1029/98JD00923, 1998.

Fletcher, S. E. M., Tans, P. P., Bruhwiler, L. M., Miller, J. B., and Heimann, M.: CH_4 sources estimated from atmospheric observations of CH_4 and its $^{13}C/^{12}C$ isotopic ratios: 2. Inverse modeling of CH_4 fluxes from geographical regions, Global Biogeochemical Cycles, 18, https://doi.org/10.1029/2004GB002224, 2004.

Folberth, G. A., Hauglustaine, D. A., Lathière, J., and Brocheton, F.: Interactive chemistry in the Laboratoire de Météorologie Dynamique general circulation model: model description and impact analysis of biogenic hydrocarbons on tropospheric chemistry, Atmospheric Chemistry and Physics, 6, 2273–2319, https://doi.org/10.5194/acp-6-2273-2006, 2006.

Fujita, R., Morimoto, S., Maksyutov, S., Kim, H.-S., Arshinov, M., Brailsford, G., Aoki, S., and Nakazawa, T.: Global and Regional CH_4 Emissions for 1995–2013 Derived From Atmospheric CH_4, $\delta^{13}C$-CH_4, and δD-CH_4 Observations and a Chemical Transport Model, Journal of Geophysical Research: Atmospheres, 125, e2020JD032 903, https://doi.org/doi.org/10.1029/2020JD032903, 2020.

Ganesan, A. L., Stell, A. C., Gedney, N., Comyn-Platt, E., Hayman, G., Rigby, M., Poulter, B., and Hornibrook, E. R. C.: Spatially Resolved Isotopic Source Signatures of Wetland Methane Emissions, Geophysical Research Letters, 45, 3737–3745, https://doi.org/10.1002/2018GL077536, 2018.

770 Gromov, S., Brenninkmeijer, C. A. M., and Jöckel, P.: A very limited role of tropospheric chlorine as a sink of the greenhouse gas methane, Atmospheric Chemistry and Physics, 18, 9831–9843, https://doi.org/doi.org/10.5194/acp-18-9831-2018, 2018.

Gupta, M., Tyler, S., and Cicerone, R.: Modeling atmospheric $\delta^{13}CH_4$ and the causes of recent changes in atmospheric CH_4 amounts, Journal of Geophysical Research: Atmospheres, 101, 22 923–22 932, https://doi.org/10.1029/96JD02386, 1996.

Hauglustaine, D. A., Hourdin, F., Jourdain, L., Filiberti, M.-A., Walters, S., Lamarque, J.-F., and Holland, E. A.: Interactive chemistry in
775 the Laboratoire de Météorologie Dynamique general circulation model: Description and background tropospheric chemistry evaluation, Journal of Geophysical Research: Atmospheres, 109, https://doi.org/10.1029/2003JD003957, 2004.

Hauglustaine, D. A., Cozic, A., Caubel, A., Lathière, J., Sépulchre, P., Cohen, Y., Balkanski, Y., Lurton, T., Boucher, O., and Tsigaridis, K.: Coupled Climate-Chemistry-Aerosol simulations under the AerChemMIP scenarios with the IPSL-CM5A2-INCA climate model, in preparation, 2021.

780 Hossaini, R., Chipperfield, M. P., Saiz-Lopez, A., Fernandez, R., Monks, S., Feng, W., Brauer, P., and von Glasow, R.: A global model of tropospheric chlorine chemistry: Organic versus inorganic sources and impact on methane oxidation, Journal of Geophysical Research: Atmospheres, 121, 14,271–14,297, https://doi.org/10.1002/2016JD025756, 2016.

Hourdin, F., Musat, I., Bony, S., Braconnot, P., Codron, F., Dufresne, J.-L., Fairhead, L., Filiberti, M.-A., Friedlingstein, P., Grandpeix, J.-Y., Krinner, G., LeVan, P., Li, Z.-X., and Lott, F.: The LMDZ4 general circulation model: climate performance and sensitivity to parametrized
785 physics with emphasis on tropical convection, Climate Dynamics, 27, 787–813, https://doi.org/10.1007/s00382-006-0158-0, 2006.

Houweling, S., Bergamaschi, P., Chevallier, F., Heimann, M., Kaminski, T., Krol, M., Michalak, A. M., and Patra, P.: Global inverse modeling of CH_4 sources and sinks: an overview of methods, Atmospheric Chemistry and Physics, 17, 235–256, https://doi.org/doi.org/10.5194/acp-17-235-2017, 2017.

Karion, A., Sweeney, C., Tans, P., and Newberger, T.: AirCore: An Innovative Atmospheric Sampling System, Journal of Atmospheric and
790 Oceanic Technology, 27, 1839–1853, https://doi.org/10.1175/2010JTECHA1448.1, 2010.

Lassey, K. R., Lowe, D. C., and Manning, M. R.: The trend in atmospheric methane $\delta^{13}C$ and implications for isotopic constraints on the global methane budget, Global Biogeochemical Cycles, 14, 41–49, https://doi.org/10.1029/1999GB900094, 2000.

Locatelli, R., Bousquet, P., Hourdin, F., Saunois, M., Cozic, A., Couvreux, F., Grandpeix, J.-Y., Lefebvre, M.-P., Rio, C., Bergamaschi, P., Chambers, S. D., Karstens, U., Kazan, V., van der Laan, S., Meijer, H. A. J., Moncrieff, J., Ramonet, M., Scheeren, H. A., Schlosser,
795 C., Schmidt, M., Vermeulen, A., and Williams, A. G.: Atmospheric transport and chemistry of trace gases in LMDz5B: evaluation and implications for inverse modelling, Geoscientific Model Development, 8, 129–150, https://doi.org/10.5194/gmd-8-129-2015, 2015.

Louis, J.-F.: A parametric model of vertical eddy fluxes in the atmosphere, Boundary-Layer Meteorology, 17, 187–202, https://doi.org/10.1007/BF00117978, 1979.

Mailler, S., Menut, L., Khvorostyanov, D., Valari, M., Couvidat, F., Siour, G., Turquety, S., Briant, R., Tuccella, P., Bessagnet, B., Colette,
800 A., Létinois, L., Markakis, K., and Meleux, F.: CHIMERE-2017: from urban to hemispheric chemistry-transport modeling, Geoscientific Model Development, 10, 2397–2423, https://doi.org/10.5194/gmd-10-2397-2017, 2017.

McCarthy, M. C., Connell, P., and Boering, K. A.: Isotopic fractionation of methane in the stratosphere and its effect on free tropospheric isotopic compositions, Geophysical Research Letters, 28, 3657–3660, https://doi.org/10.1029/2001GL013159, 2001.

McCarthy, M. C., Boering, K. A., Rice, A. L., Tyler, S. C., Connell, P., and Atlas, E.: Carbon and hydrogen isotopic compositions of stratospheric methane: 2. Two-dimensional model results and implications for kinetic isotope effects, Journal of Geophysical Research: Atmospheres, 108, https://doi.org/10.1029/2002JD003183, 2003.

McNorton, J., Wilson, C., Gloor, M., Parker, R. J., Boesch, H., Feng, W., Hossaini, R., and Chipperfield, M. P.: Attribution of recent increases in atmospheric methane through 3-D inverse modelling, Atmospheric Chemistry and Physics, 18, 18 149–18 168, https://doi.org/doi.org/10.5194/acp-18-18149-2018, 2018.

Meinshausen, M., Vogel, E., Nauels, A., Lorbacher, K., Meinshausen, N., Etheridge, D. M., Fraser, P. J., Montzka, S. A., Rayner, P. J., Trudinger, C. M., Krummel, P. B., Beyerle, U., Canadell, J. G., Daniel, J. S., Enting, I. G., Law, R. M., Lunder, C. R., O'Doherty, S., Prinn, R. G., Reimann, S., Rubino, M., Velders, G. J. M., Vollmer, M. K., Wang, R. H. J., and Weiss, R.: Historical greenhouse gas concentrations for climate modelling (CMIP6), Geoscientific Model Development, 10, 2057–2116, https://doi.org/doi.org/10.5194/gmd-10-2057-2017, 2017.

Membrive, O., Crevoisier, C., Sweeney, C., Danis, F., Hertzog, A., Engel, A., Bönisch, H., and Picon, L.: AirCore-HR: a high-resolution column sampling to enhance the vertical description of CH_4 and CO_2, Atmos. Meas. Tech., p. 20, 2017.

Menut, L., Bessagnet, B., Khvorostyanov, D., Beekmann, M., Blond, N., Colette, A., Coll, I., Curci, G., Foret, G., Hodzic, A., Mailler, S., Meleux, F., Monge, J.-L., Pison, I., Siour, G., Turquety, S., Valari, M., Vautard, R., and Vivanco, M. G.: CHIMERE 2013: a model for regional atmospheric composition modelling, Geoscientific Model Development, 6, 981–1028, https://doi.org/10.5194/gmd-6-981-2013, 2013.

Monteil, G., Houweling, S., Dlugockenky, E. J., Maenhout, G., Vaughn, B. H., White, J. W. C., and Rockmann, T.: Interpreting methane variations in the past two decades using measurements of CH_4 mixing ratio and isotopic composition, Atmospheric Chemistry and Physics, 11, 9141–9153, https://doi.org/doi.org/10.5194/acp-11-9141-2011, 2011.

Müller, R., Brenninkmeijer, C. A. M., and Crutzen, P. J.: A large [13]CO deficit in the lower Antarctic stratosphere due to "ozone hole" chemistry: Part II, Modeling, Geophysical Research Letters, 23, 2129–2132, https://doi.org/10.1029/96GL01472, 1996.

Neef, L., Weele, M. v., and Velthoven, P. v.: Optimal estimation of the present-day global methane budget, Global Biogeochemical Cycles, 24, https://doi.org/10.1029/2009GB003661, 2010.

Nisbet, E. G., Manning, M. R., Dlugokencky, E. J., Fisher, R. E., Lowry, D., Michel, S. E., Myhre, C. L., Platt, S. M., Allen, G., Bousquet, P., Brownlow, R., Cain, M., France, J. L., Hermansen, O., Hossaini, R., Jones, A. E., Levin, I., Manning, A. C., Myhre, G., Pyle, J. A., Vaughn, B. H., Warwick, N. J., and White, J. W. C.: Very Strong Atmospheric Methane Growth in the 4 Years 2014–2017: Implications for the Paris Agreement, Global Biogeochemical Cycles, 33, 318–342, https://doi.org/10.1029/2018GB006009, 2019.

Ostler, A., Sussmann, R., Patra, P. K., Houweling, S., Bruine, M. D., Stiller, G. P., Haenel, F. J., Plieninger, J., Bousquet, P., Yin, Y., Saunois, M., Walker, K. A., Deutscher, N. M., Griffith, D. W. T., Blumenstock, T., Hase, F., Warneke, T., Wang, Z., Kivi, R., and Robinson, J.: Evaluation of column-averaged methane in models and TCCON with a focus on the stratosphere, Atmospheric Measurement Techniques, 9, 4843–4859, https://doi.org/doi.org/10.5194/amt-9-4843-2016, 2016.

Patra, P. K., Houweling, S., Krol, M., Bousquet, P., Belikov, D., Bergmann, D., Bian, H., Cameron-Smith, P., Chipperfield, M. P., Corbin, K., Fortems-Cheiney, A., Fraser, A., Gloor, E., Hess, P., Ito, A., Kawa, S. R., Law, R. M., Loh, Z., Maksyutov, S., Meng, L., Palmer, P. I., Prinn, R. G., Rigby, M., Saito, R., and Wilson, C.: TransCom model simulations of CH_4 and related species: linking transport, surface flux and chemical loss with CH_4 variability in the troposphere and lower stratosphere, Atmospheric Chemistry and Physics, 11, 12 813–12 837, https://doi.org/10.5194/acp-11-12813-2011, 2011.

Pison, I., Bousquet, P., Chevallier, F., Szopa, S., and Hauglustaine, D.: Multi-species inversion of CH_4, CO and H_2 emissions from surface measurements, Atmos. Chem. Phys., p. 17, 2009.

Rice, A. L., Tyler, S. C., McCarthy, M. C., Boering, K. A., and Atlas, E.: Carbon and hydrogen isotopic compositions of stratospheric methane: 1. High-precision observations from the NASA ER-2 aircraft, Journal of Geophysical Research: Atmospheres, 108, https://doi.org/10.1029/2002JD003042, 2003.

Rice, A. L., Butenhoff, C. L., Teama, D. G., Röger, F. H., Khalil, M. A. K., and Rasmussen, R. A.: Atmospheric methane isotopic record favors fossil sources flat in 1980s and 1990s with recent increase, Proceedings of the National Academy of Sciences, 113, 10791–10796, https://doi.org/10.1073/pnas.1522923113, 2016.

Rigby, M., Manning, A. J., and Prinn, R. G.: The value of high-frequency, high-precision methane isotopologue measurements for source and sink estimation, Journal of Geophysical Research: Atmospheres, 117, https://doi.org/10.1029/2011JD017384, 2012.

Röckmann, T., Grooß, J.-U., and Müller, R.: The impact of anthropogenic chlorine emissions, stratospheric ozone change and chemical feedbacks on stratospheric water, Atmospheric Chemistry and Physics, 4, 693–699, https://doi.org/10.5194/acp-4-693-2004, 2004.

Röckmann, T., Brass, M., Borchers, R., and Engel, A.: The isotopic composition of methane in the stratosphere: high-altitude balloon sample measurements, Atmospheric Chemistry and Physics, 11, 13287–13304, https://doi.org/doi.org/10.5194/acp-11-13287-2011, 2011.

Saueressig, G., Bergamaschi, P., Crowley, J. N., Fischer, H., and Harris, G. W.: Carbon kinetic isotope effect in the reaction of CH_4 with Cl atoms, Geophysical Research Letters, 22, 1225–1228, https://doi.org/10.1029/95GL00881, 1995.

Saueressig, G., Crowley, J. N., Bergamaschi, P., Brühl, C., Brenninkmeijer, C. A. M., and Fischer, H.: Carbon 13 and D kinetic isotope effects in the reactions of CH_4 with $O(^1D)$ and OH: New laboratory measurements and their implications for the isotopic composition of stratospheric methane, Journal of Geophysical Research: Atmospheres, 106, 23127–23138, https://doi.org/10.1029/2000JD000120, 2001.

Saunois, M., Stavert, A. R., Poulter, B., Bousquet, P., Canadell, J. G., Jackson, R. B., Raymond, P. A., Dlugokencky, E. J., Houweling, S., Patra, P. K., Ciais, P., Arora, V. K., Bastviken, D., Bergamaschi, P., Blake, D. R., Brailsford, G., Bruhwiler, L., Carlson, K. M., Carrol, M., Castaldi, S., Chandra, N., Crevoisier, C., Crill, P. M., Covey, K., Curry, C. L., Etiope, G., Frankenberg, C., Gedney, N., Hegglin, M. I., Höglund-Isaksson, L., Hugelius, G., Ishizawa, M., Ito, A., Janssens-Maenhout, G., Jensen, K. M., Joos, F., Kleinen, T., Krummel, P. B., Langenfelds, R. L., Laruelle, G. G., Liu, L., Machida, T., Maksyutov, S., McDonald, K. C., McNorton, J., Miller, P. A., Melton, J. R., Morino, I., Müller, J., Murguia-Flores, F., Naik, V., Niwa, Y., Noce, S., O'Doherty, S., Parker, R. J., Peng, C., Peng, S., Peters, G. P., Prigent, C., Prinn, R., Ramonet, M., Regnier, P., Riley, W. J., Rosentreter, J. A., Segers, A., Simpson, I. J., Shi, H., Smith, S. J., Steele, L. P., Thornton, B. F., Tian, H., Tohjima, Y., Tubiello, F. N., Tsuruta, A., Viovy, N., Voulgarakis, A., Weber, T. S., van Weele, M., van der Werf, G. R., Weiss, R. F., Worthy, D., Wunch, D., Yin, Y., Yoshida, Y., Zhang, W., Zhang, Z., Zhao, Y., Zheng, B., Zhu, Q., Zhu, Q., and Zhuang, Q.: The Global Methane Budget 2000–2017, Earth System Science Data, 12, 1561–1623, https://doi.org/doi.org/10.5194/essd-12-1561-2020, 2020.

Schaefer, H., Fletcher, S. E. M., Veidt, C., Lassey, K. R., Brailsford, G. W., Bromley, T. M., Dlugokencky, E. J., Michel, S. E., Miller, J. B., Levin, I., Lowe, D. C., Martin, R. J., Vaughn, B. H., and White, J. W. C.: A 21st-century shift from fossil-fuel to biogenic methane emissions indicated by $^{13}CH_4$, Science, 352, 80–84, https://doi.org/10.1126/science.aad2705, 2016.

Schwietzke, S., Sherwood, O. A., Bruhwiler, L. M. P., Miller, J. B., Etiope, G., Dlugokencky, E. J., Michel, S. E., Arling, V. A., Vaughn, B. H., White, J. W. C., and Tans, P. P.: Upward revision of global fossil fuel methane emissions based on isotope database, Nature, 538, 88–91, https://doi.org/10.1038/nature19797, 2016.

Sherwen, T., Evans, M. J., Carpenter, L. J., Andrews, S. J., Lidster, R. T., Dix, B., Koenig, T. K., Sinreich, R., Ortega, I., Volkamer, R., Saiz-Lopez, A., Prados-Roman, C., Mahajan, A. S., and Ordóñez, C.: Iodine's impact on tropospheric oxidants: a global model study in GEOS-Chem, Atmospheric Chemistry and Physics, 16, 1161–1186, https://doi.org/10.5194/acp-16-1161-2016, publisher: Copernicus GmbH, 2016a.

Sherwen, T., Schmidt, J. A., Evans, M. J., Carpenter, L. J., Großmann, K., Eastham, S. D., Jacob, D. J., Dix, B., Koenig, T. K., Sinreich, R., Ortega, I., Volkamer, R., Saiz-Lopez, A., Prados-Roman, C., Mahajan, A. S., and Ordóñez, C.: Global impacts of tropospheric halogens (Cl, Br, I) on oxidants and composition in GEOS-Chem, Atmospheric Chemistry and Physics, 16, 12239–12271, https://doi.org/doi.org/10.5194/acp-16-12239-2016, 2016b.

Sherwood, O. A., Schwietzke, S., Arling, V. A., and Etiope, G.: Global Inventory of Gas Geochemistry Data from Fossil Fuel, Microbial and Burning Sources, version 2017, Earth System Science Data, 9, 639–656, https://doi.org/10.5194/essd-9-639-2017, 2017.

Stolper, D. A., Sessions, A. L., Ferreira, A. A., Santos Neto, E. V., Schimmelmann, A., Shusta, S. S., Valentine, D. L., and Eiler, J. M.: Combined ^{13}C–D and D–D clumping in methane: Methods and preliminary results, Geochimica et Cosmochimica Acta, 126, 169–191, https://doi.org/10.1016/j.gca.2013.10.045, 2014.

Strode, S. A., Wang, J. S., Manyin, M., Duncan, B., Hossaini, R., Keller, C. A., Michel, S. E., and White, J. W. C.: Strong sensitivity of the isotopic composition of methane to the plausible range of tropospheric chlorine, Atmospheric Chemistry and Physics, 20, 8405–8419, https://doi.org/10.5194/acp-20-8405-2020, 2020.

Takigawa, M., Takahashi, M., and Akiyoshi, H.: Simulation of ozone and other chemical species using a Center for Climate System Research/National Institute for Environmental Studies atmospheric GCM with coupled stratospheric chemistry, Journal of Geophysical Research: Atmospheres, 104, 14003–14018, https://doi.org/10.1029/1998JD100105, 1999.

Terrenoire, E., Hauglustaine, D., Cohen, Y., Cozic, A., Valorso, R., Lefèvre, F., and Matthes, S.: Impact of present and future aircraft NO$_x$ and aerosol emissions on atmospheric composition and associated direct radiative forcing of climate, Atmospheric Chemistry and Physics Discussions, 2022, 1–39, https://doi.org/10.5194/acp-2022-222, 2022.

Thanwerdas, J., Saunois, M., Berchet, A., Pison, I., Vaughn, B. H., Michel, S. E., and Bousquet, P.: Variational inverse modelling within the Community Inversion Framework to assimilate δ^{13}C(CH$_4$) and CH$_4$: a case study with model LMDz-SACS, Geoscientific Model Development Discussions, pp. 1–29, https://doi.org/10.5194/gmd-2021-106, 2021.

Thompson, R. L., Nisbet, E. G., Pisso, I., Stohl, A., Blake, D., Dlugokencky, E. J., Helmig, D., and White, J. W. C.: Variability in Atmospheric Methane From Fossil Fuel and Microbial Sources Over the Last Three Decades, Geophysical Research Letters, 45, 11,499–11,508, https://doi.org/10.1029/2018GL078127, 2018.

Tiedtke, M.: A Comprehensive Mass Flux Scheme for Cumulus Parameterization in Large-Scale Models, Monthly Weather Review, 117, 1779–1800, https://doi.org/10.1175/1520-0493(1989)117<1779:ACMFSF>2.0.CO;2, 1989.

Wang, J. S., McElroy, M. B., Spivakovsky, C. M., and Jones, D. B. A.: On the contribution of anthropogenic Cl to the increase in δ^{13}C of atmospheric methane: ANTHROPOGENIC Cl AND δ^{13}C OF METHANE, Global Biogeochemical Cycles, 16, 20–1–20–11, https://doi.org/10.1029/2001GB001572, 2002.

Wang, X., Jacob, D. J., Eastham, S. D., Sulprizio, M. P., Zhu, L., Chen, Q., Alexander, B., Sherwen, T., Evans, M. J., Lee, B. H., Haskins, J. D., Lopez-Hilfiker, F. D., Thornton, J. A., Huey, G. L., and Liao, H.: The role of chlorine in global tropospheric chemistry, Atmospheric Chemistry and Physics, 19, 3981–4003, https://doi.org/10.5194/acp-19-3981-2019, 2019.

Wang, X., Jacob, D. J., Fu, X., Wang, T., Breton, M. L., Hallquist, M., Liu, Z., McDuffie, E. E., and Liao, H.: Effects of Anthropogenic Chlorine on PM $_{2.5}$ and Ozone Air Quality in China, Environmental Science & Technology, 54, 9908–9916, https://doi.org/10.1021/acs.est.0c02296, 2020.

Wang, X., Jacob, D. J., Downs, W., Zhai, S., Zhu, L., Shah, V., Holmes, C. D., Sherwen, T., Alexander, B., Evans, M. J., Eastham, S. D., Neuman, J. A., Veres, P., Koenig, T. K., Volkamer, R., Huey, L. G., Bannan, T. J., Percival, C. J., Lee, B. H., and Thornton, J. A.: Global tropospheric halogen (Cl, Br, I) chemistry and its impact on oxidants, Atmospheric Chemistry and Physics Discussions, pp. 1–34, https://doi.org/10.5194/acp-2021-441, 2021.

Warwick, N. J., Cain, M. L., Fisher, R., France, J. L., Lowry, D., Michel, S. E., Nisbet, E. G., Vaughn, B. H., White, J. W. C., and Pyle, J. A.: Using δ^{13}C-CH$_4$ and deltaD-CH$_4$ to constrain Arctic methane emissions, Atmospheric Chemistry and Physics, 16, 14 891–14 908, https://doi.org/10.5194/acp-16-14891-2016, 2016.

White, J. W. C., Vaughn, B. H., and Michel, S. E.: Stable isotopic composition of atmospheric methane (^{13}C) from the NOAA ESRL Carbon Cycle Cooperative Global Air Sampling Network, 1998–2018, available at ftp://aftp.cmdl.noaa.gov/data/trace_gases/ch4c13/flask/., last access: 12 July 2021, 2021.

Zhao, Y., Saunois, M., Bousquet, P., Lin, X., Berchet, A., Hegglin, M. I., Canadell, J. G., Jackson, R. B., Hauglustaine, D. A., Szopa, S., Stavert, A. R., Abraham, N. L., Archibald, A. T., Bekki, S., Deushi, M., Jöckel, P., Josse, B., Kinnison, D., Kirner, O., Marécal, V., O'Connor, F. M., Plummer, D. A., Revell, L. E., Rozanov, E., Stenke, A., Strode, S., Tilmes, S., Dlugokencky, E. J., and Zheng, B.: Inter-model comparison of global hydroxyl radical (OH) distributions and their impact on atmospheric methane over the 2000–2016 period, Atmospheric Chemistry and Physics, 19, 13 701–13 723, https://doi.org/10.5194/acp-19-13701-2019, 2019.

Zhao, Y., Saunois, M., Bousquet, P., Lin, X., Berchet, A., Hegglin, M. I., Canadell, J. G., Jackson, R. B., Dlugokencky, E. J., Langenfelds, R. L., Ramonet, M., Worthy, D., and Zheng, B.: Influences of hydroxyl radicals (OH) on top-down estimates of the global and regional methane budgets, Atmospheric Chemistry and Physics, 20, 9525–9546, https://doi.org/doi.org/10.5194/acp-20-9525-2020, 2020.
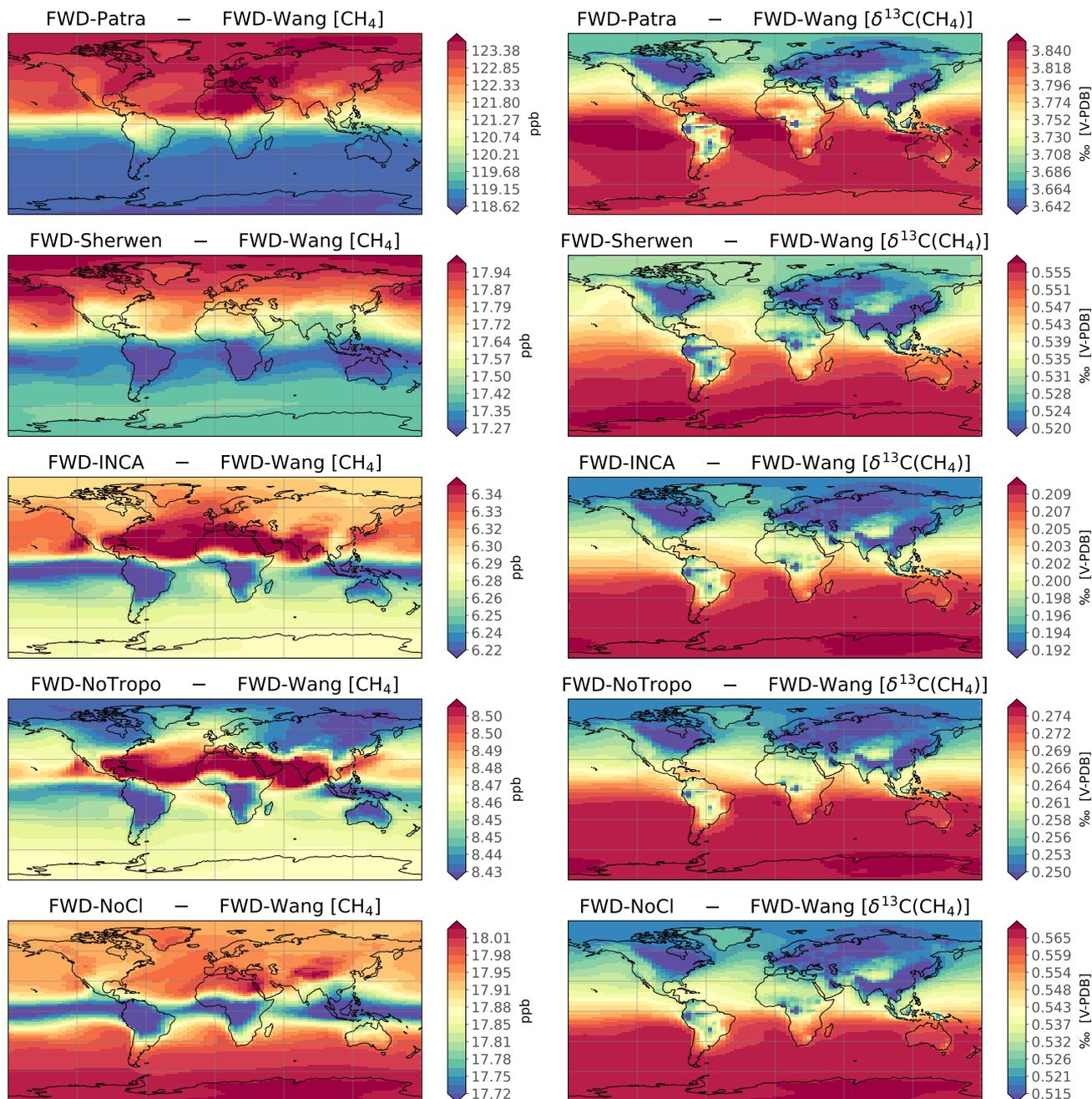
Figure 2. Surface absolute bias between FWD-* and FWD-Wang simulations averaged over 2010-2018. Temporal average is performed before substraction. First column displays the biases between CH_4 mole fractions. Second column shows the biases between $\delta^{13}C(CH_4)$ values. Note that the scales are different for each panel.
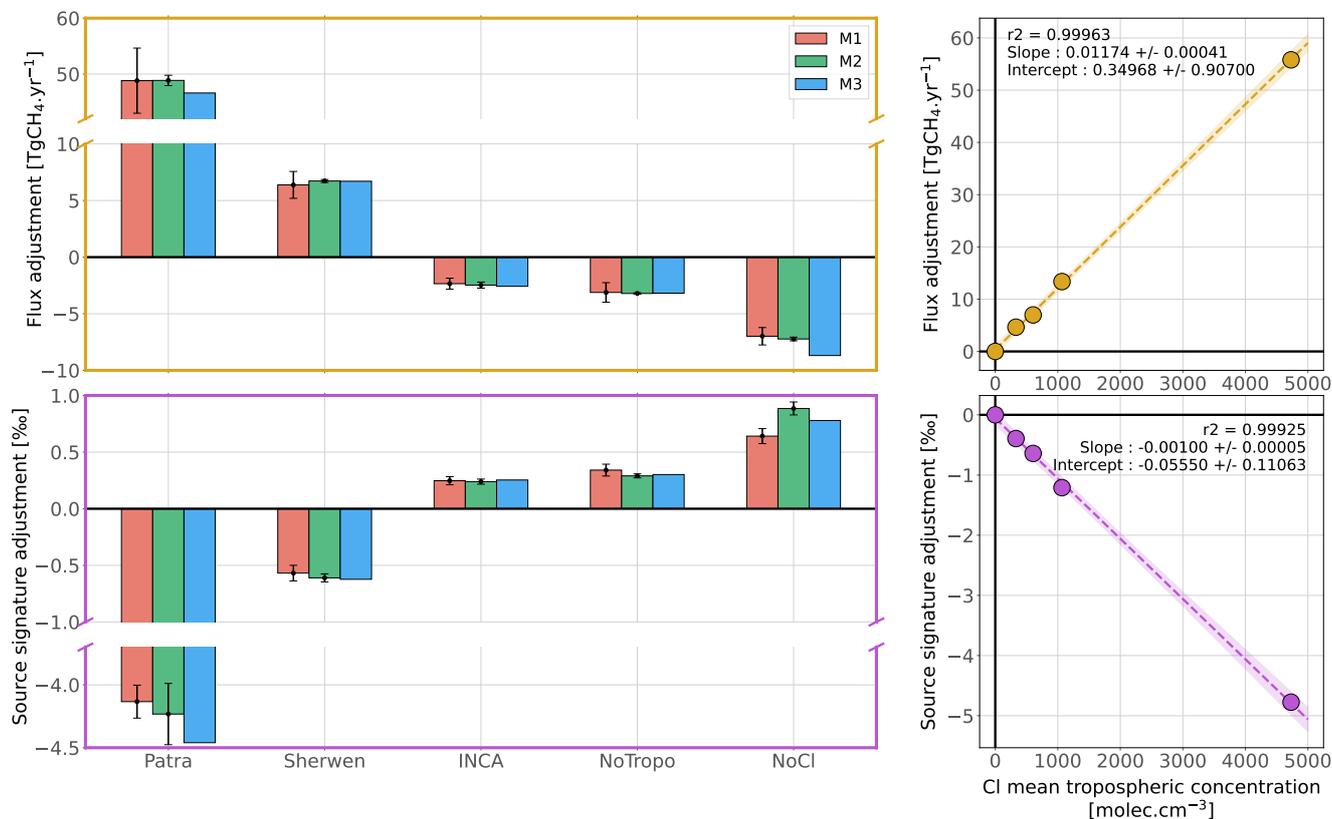
Figure 3. Global CH$_4$ flux and δ^{13}C(CH$_4$)$_{source}$ source signature adjustment due to a change in the prescribed Cl field. Left panels show the adjustments for global CH$_4$ flux (upper panel) and δ^{13}C(CH$_4$)$_{source}$ source signature (lower panel), with multiple methods (M1, M2 and M3) presented in Sect. 2.5 and supplementary Text S1, S2 and S3. Simulations with Cl-Wang are taken as a reference. For M1 and M2, the error bars correspond to the inter-annual variations (one standard deviation) of adjustments. Right panels display the linear model derived from the relationship between the adjustments (estimated with M1) and the mean tropospheric concentration of the prescribed Cl fields. For the linear regression only, simulations without the Cl sink (NoCl) are taken as a reference to calculate the adjustments.
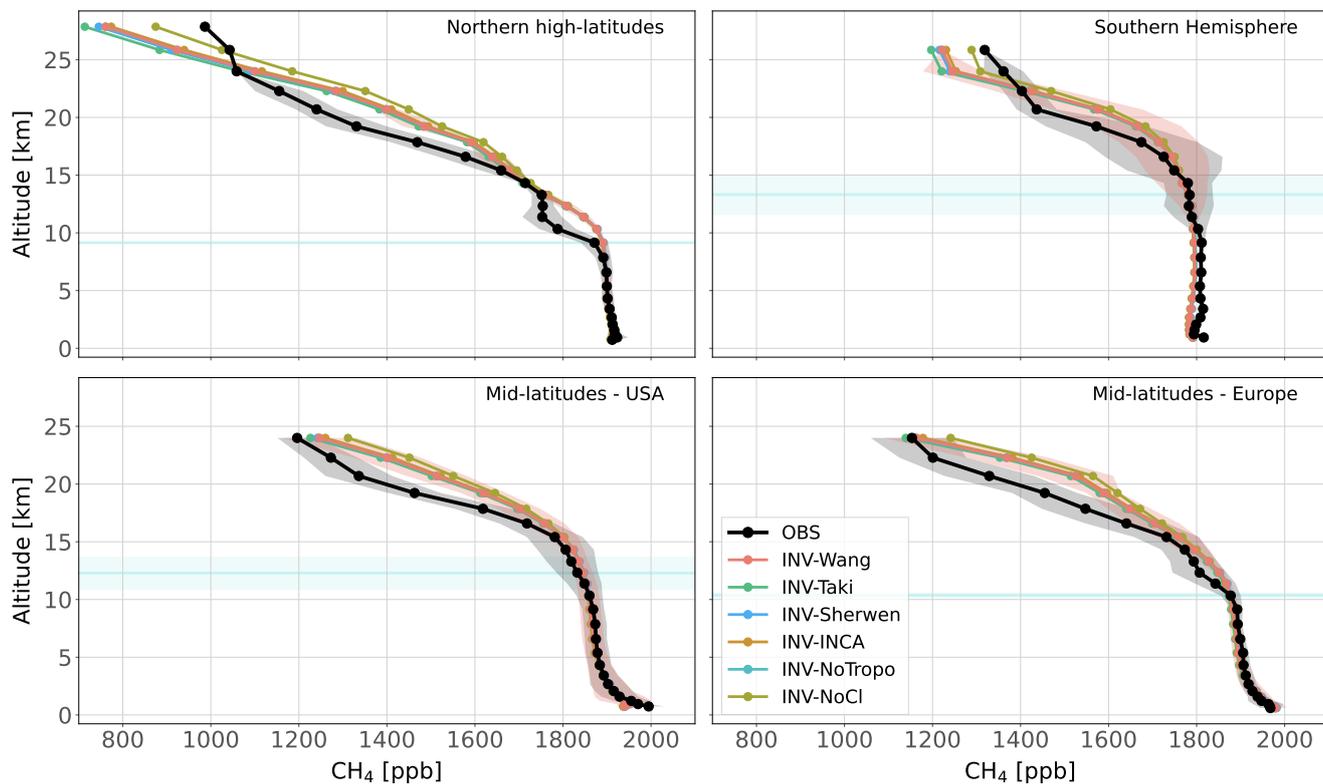
Figure 4. Observed and simulated CH_4 vertical profiles for four regions. All available vertical profiles in each region have been averaged. Shaded areas indicate the standard deviations of this average. Blue line and its associated shaded area show the mean altitude of the tropopause and its standard deviation over the vertical profiles in the region.
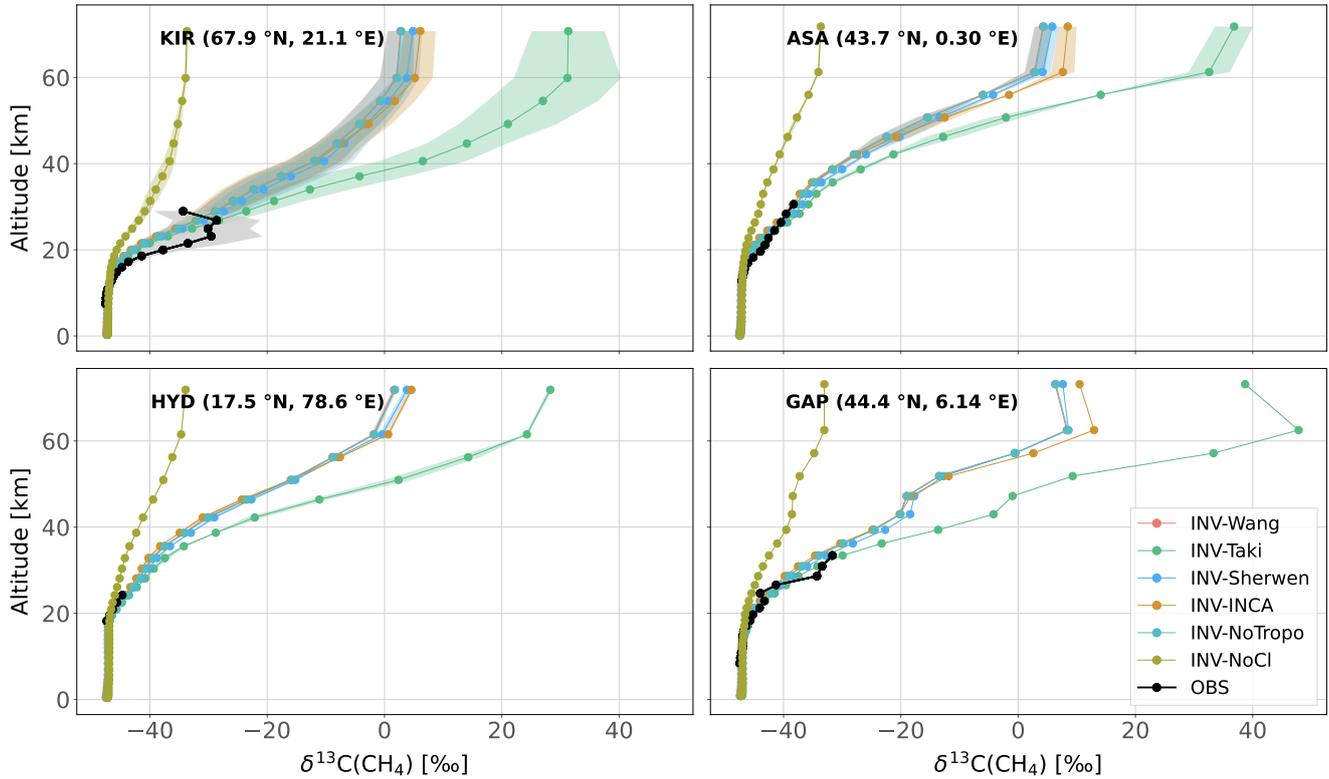
Figure 5. Observed and simulated $\delta^{13}C(CH_4)$ vertical profiles for ~~the Northern Hemisphere (left panel) and Southern Hemisphere (right panel)~~four locations. All available vertical profiles in each region have been averaged. Shaded areas indicate the standard deviations of this average. Note that measurement uncertainties (around 0.2 ‰) are much lower than the x-axis range. KIR : Kiruna, Sweden (67.9 °N, 21.10 °E) ; ASA : Aire sur l'Adour, France (43.70 °N, 0.30 °E) ; HYD : Hyderabad, India (17.5 °N, 78.60 °E) ; GAP : Gap, France (44.44 °N, 6.14 °E).